

# Probability Distributions of Line Lattices in Random Media from the 1D Bose Gas

Thorsten Emig<sup>a,1</sup> and Mehran Kardar<sup>a,b,2</sup>

<sup>a</sup>*Physics Department, Massachusetts Institute of Technology,  
Cambridge, MA 02139, USA*

<sup>b</sup>*Institute for Theoretical Physics, University of California,  
Santa Barbara, CA 93106, USA*

---

## Abstract

The statistical properties of a two dimensional lattice of elastic lines in a random medium are studied using the Bethe ansatz. We present a novel mapping of the dilute random line lattice onto the weak coupling limit of a pure Bose gas with delta-function interactions. Using this mapping, we calculate the cumulants of the free energy in the dilute limit exactly. The relation between density and displacement correlation functions in the two models is examined and compared with existing results from renormalization group and variational ansätze.

*PACS:* 05.30.-d, 05.70.-a, 64.60.Cn, 74.60.Ge

---

## 1 Introduction

Disorder, in the form of quenched impurities in a sample, is likely to modify various measurements. However, from a theoretical point of view, characterizing the behavior of disordered systems has proven difficult, making this one of the most challenging and controversial fields of statistical mechanics. The directed polymer in a random medium (DPRM) is one of the rare cases of a disorder-dominated system whose statistical properties can be determined in great detail both analytically and numerically [1], and thus serves as a prototype for other such systems. Furthermore, its behavior is related to a plethora of other problems in statistical mechanics, such as the kinetic roughening of surfaces [2], the hydrodynamics of the Burger's equations [3], and surprisingly the biological sequence-alignment problem for genes and proteins [4,5].

---

<sup>1</sup> E-mail: emig@mit.edu

<sup>2</sup> E-mail: kardar@mit.edu

The DPRM is directly relevant to vortex lines in superconductors with point impurities. Most research on the vortex phases in these systems has focused on the structural properties of the flux lattice in a sample containing many vortices. Recently, the statistics of single vortex lines was studied experimentally on a two dimensional flux line lattice oriented parallel to a thin micrometer-sized film of 2H-NbSe<sub>2</sub> [6]. Magnetic response measurements show interesting sample dependent fine structure in the constitutive relation  $B(H)$ , providing a fingerprint of the underlying random pinning landscape. More generally, the random potential is expected to modify the measurement of various thermodynamic and structural quantities, making it desirable to characterize the probability distribution functions (PDFs) for the outcome. At one extreme, microscopic quantities such as two-point correlation functions are quite sensitive to randomness, inducing in some cases complicated multiscaling behavior of their PDFs [7]. On the other hand, the free energy and other macroscopic quantities are expected to have simpler self-averaging behavior, while non-trivial finite-size effects are still present in their corresponding PDFs.

To date, the PDF of the free energy is known exactly only for a single line, the DPRM [8–11]. However, as in superconductors, in most cases elastic lines appear at a finite density, leading to novel effects resulting from a competition between randomness and line interactions. Similar line lattice structures occur in domain walls in the incommensurate phase of charge-density-waves, in monolayers adsorbed on crystal surfaces, and in the form of steps on the vicinal surface of a crystal [12]. As pointed out by de Gennes in the context of polymers [13], and later on by Pokrovsky and Talapov for domain walls in incommensurate phases [14], the statistical mechanics of a *pure* two-dimensional line lattice maps onto one-dimensional free fermions if the repulsive line interactions are replaced by non-crossing constraints. Applying the same constraint, Kardar used the replica method to show that the line lattice in a random potential maps onto one-dimensional  $U(n)$  fermions with an attractive interaction [8]. Calculating the ground state energy of this quantum system for integer  $n$  by Bethe ansatz, and analytically continuing to  $n \rightarrow 0$ , the quench-averaged free energy was calculated in this reference. Although the PDF was not calculated explicitly, a scaling ansatz for the replica free energy was proposed based on dimensional arguments. Following up on this mapping, there have been attempts [15,16] to calculate the density correlations of the line lattice from the excitation spectrum of the  $U(n)$  fermions by Bethe ansatz, leading to different results.

In this paper we examine the analogy between the replicated line lattice and  $U(n)$  fermions further. A considerable difficulty in the replica approach is the need for analytical continuation to small  $n$  of the results obtained for integer  $n$ . Analyticity is usually assumed in replica theories, since it cannot be proved in most cases. Here we develop a new method for analytical continuation in the line lattice problem which is based on Euler’s gamma function, the natural

continuation of the factorial to real valued arguments. This technique provides an analytic expression for the replica free energy of the line lattice at small  $n$  in terms of an integral equation, which in general has to be solved numerically. Interestingly, in the dilute limit of the line lattice, the analytically continued Bethe ansatz equations are identical to that of the 1D Bose gas with delta-function repulsions. This novel mapping allows us to obtain exact expressions for the free energy cumulants of the line lattice, and to reveal new relations between density correlations in the 1D Bose gas and the replica theory of the line lattice, respectively. The scaling predictions for the replica free energy proposed in [8], and used in [17] in a wider context of disordered systems, are strikingly confirmed.

The outline of the paper is as follows. Using the replica method and the analogy between elastic lines and world-line of quantum particles, we first show that the random line system is described by a quantum problem of “colored” fermions, which interact upon contact. This analogy is explained in detail in Section 2. Exact solutions for the ground state energy of this colored fermion model in the thermodynamic limit are then obtained via the series of nested Bethe ansätze introduced by Yang [18]. For an integer number  $n$  of colors, the resulting sets of Bethe ansatz equations can be reduced to a single set of equations by considering  $n$ -clusters of fermions, as showed by Takahashi [19] and Kardar [8]. These integer  $n$  equations are derived in Subsection 3.1. In the following Subsection 3.2, we develop a new technique to continue the discrete Bethe ansatz equations directly to continuous  $n$ . We find that for small  $n$ , and in the limit of low line density, the complex  $n$ -color fermion problem can be mapped onto the well-studied one-dimensional Bose gas with delta-function repulsions [20] (see Section 4). It turns out that the Bose gas interaction strength is proportional to the number  $n$  of replicas, thus mapping the interesting regime  $n \ll 1$  into the weak coupling limit of the Bose gas. Therefore, the problem of calculating disorder averaged cumulants of the free energy of the line system becomes equivalent to a perturbative expansion of the ground state energy of the one-dimensional Bose gas in the weak coupling limit. The exact results for the cumulants of the free energy are presented in Section 5. Finally, in Section 6 we apply our novel mapping to the question of what can be learned about the density-density correlation function of the line lattice from the known results for corresponding correlation functions of the 1D Bose gas.

## 2 Mapping fluctuating lines to fermions

Configurations of directed elastic lines can be regarded as the world lines of quantum particles, where the coordinate along the line plays the role of time. To develop a concrete picture of this analogy, we consider the canonical parti-

tion sum  $Z_N$  of a  $1 + 1$  dimensional lattice of  $N$  interacting lines in a random environment of lateral length  $L$ . To simplify the sum over all configurations of the lines, we assume periodic boundary conditions in the direction parallel to the lines. This is justified since the statistical mechanics of the line lattice is insensitive to the particular choice of boundary conditions in the limit where  $L$  is much larger than the spacing between line collisions [21]. Now the partition sum can be written as the path integral

$$Z_N[V(x, y)] = \frac{\mathcal{Z}_0^N}{N!} \sum_P \prod_{j=1}^N \int dr_j \int_{x_j(0)=r_j}^{x_j(L)=r_{P_j}} \mathcal{D}x_j(y) \exp \{-H[V(x, y)]/T\}, \quad (1)$$

where we have summed over all permutations  $P$  and have used Feynman's definition of the path-integral measure  $\mathcal{D}x_j(y)$  [22]. Here  $\mathcal{Z}_0$  denotes the partition function of a single line in a pure system with only one end of the line fixed<sup>3</sup>. The Hamiltonian in Eq. (1) is given by

$$H[V(x, y)] = \int_0^L dy \left\{ \sum_{j=1}^N \frac{g}{2} \left( \frac{dx_j}{dy} \right)^2 + \sum_{i < j} U(x_i - x_j) + \sum_{j=1}^N V(x_j, y) \right\}, \quad (2)$$

which is a functional of the random potential  $V(x, y)$ . The first term measures the elastic energy of individual lines with line tension  $g$ . The lines interact via a short ranged repulsive pair potential  $U(x)$ , which is local in  $y$ . Effectively, a line interacts only with the lines in the same constant  $y$  cross section. This assumption is valid if the line coordinates  $x_j(y)$  vary slowly with  $y$ . The last term couples the potential from randomly distributed impurities to the local line positions, and makes the Hamiltonian “time” dependent. Without this last term, the expression for  $Z_N$  is formally identical to the Feynman path integral for the canonical partition sum of an interacting 1D Bose gas [21]. But there is an additional restriction for the configurations of elastic lines compared to the boson world lines. Usually the overlap of lines is associated with a high energy cost and, therefore, we treat the lines as non-crossing, corresponding to an infinite potential  $U(x)$  at  $x = 0$ . As a consequence, only the identity permutation contributes to the sum in Eq. (1).

The free energy  $F[V(x, y)] = -T \ln Z_N$  is itself a random variable. To obtain the probability distribution function (PDF) of the free energy, we use the replica method. Moments of the partition function are obtained by introducing  $n$  replicas of the original system, described by line coordinates  $x_{j,\alpha}(y)$ ,  $\alpha = 1, \dots, n$ , and then averaging over the random potential. Assuming that  $V(x, y)$  is Gaussian distributed with zero mean and spatially uncorrelated with

---

<sup>3</sup>  $\mathcal{Z}_0$  depends on the lattice constants of the discretization of the path integral. The partition function of the interacting random line system will be expressed relative to  $\mathcal{Z}_0$  [21].

variance

$$[V(x, y)V(x', y')] = \Delta\delta(x - x')\delta(y - y'), \quad (3)$$

where  $[\dots]$  denotes impurity averaging, the average over the random potential yields

$$[Z_N^n] = \frac{\mathcal{Z}_0^{nN}}{(N!)^n} \prod_{\alpha=1}^n \prod_{j=1}^N \int dr_{j,\alpha} \int_{x_{j,\alpha}(0)=r_{j,\alpha}}^{x_{j,\alpha}(L)=r_{j,\alpha}} \mathcal{D}x_{j,\alpha}(y) \exp\{-H_n/T\}, \quad (4)$$

with the replicated Hamiltonian

$$H_n = \int_0^L dy \left\{ \sum_{\alpha=1}^n \sum_{j=1}^N \frac{g}{2} \left( \frac{dx_{j,\alpha}}{dy} \right)^2 + \sum_{\alpha=1}^n \sum_{i < j} U(x_{i,\alpha}(y) - x_{j,\alpha}(y)) - \frac{\Delta}{2T} \sum_{\alpha,\beta=1}^n \sum_{i,j=1}^N \delta(x_{i,\alpha}(y) - x_{j,\beta}(y)) \right\}. \quad (5)$$

The sum over permutations has been eliminated from Eq. (4) due to the non-crossing condition. The impurity averaged moments of  $Z_N$  are obtained from the time-independent Hamiltonian  $H_n$  at the cost of introducing a new attractive interaction proportional to the variance  $\Delta$  of the random potential. This attraction can be understood as follows. In the original random system the lines prefer to wander through regions of favorable values of the random potential  $V(x, y)$ . Due to the impurity average the system becomes translationally invariant and there are no longer energetically favored regions of space-time. Instead, in calculating  $n$ th moments of  $Z_N$ , the system of  $n$  copies of the lines gains due to  $[\exp(-V(x, y))] = \exp(\Delta/2)$  an energy  $\Delta/2T$  per crossing of two lines (of different replicas), thus leading to an attraction.

The time-independence of the replicated Hamiltonian, and the choice of periodic boundary conditions, allows us to write the partition function in terms of the symmetric statistical density matrix  $\rho_{sym}(x_{1,1}, \dots, x_{N,n}; x'_{1,1}, \dots, x'_{N,n}; L)$  as an integral over all boundary positions of the lines at  $y = 0$ ,

$$[Z_N^n] = \mathcal{Z}_0^{nN} \int \prod_{j=1}^N \prod_{\alpha=1}^n dx_{j,\alpha} \rho_{sym}(x_{1,1}, \dots, x_{N,n}; x_{1,1}, \dots, x_{N,n}; L). \quad (6)$$

The density matrix itself can be written as an imaginary time Feynman path integral for the world lines of  $Nn$  particles with fixed boundary positions  $x_{1,1}, \dots, x_{N,n}$  at  $y = 0$  and  $x'_{1,1}, \dots, x'_{N,n}$  at  $y = L$  [22]. The density matrix can alternatively be expressed in coordinate representation as

$$\begin{aligned} \rho_{sym}(x_{1,1}, \dots, x_{N,n}; x'_{1,1}, \dots, x'_{N,n}; L) &= \\ &= \sum_i^{sym} e^{-\beta_{qm} E_i} \psi_i(x_{1,1}, \dots, x_{N,n}) \psi_i^*(x'_{1,1}, \dots, x'_{N,n}), \end{aligned} \quad (7)$$

with the mapping  $\beta_{qm} \rightarrow \beta_{cl} L = L/T$ ,  $\hbar \rightarrow \beta_{cl}^{-1} = T$  between quantum mechanical and classical parameters<sup>4</sup>. The sum runs over all symmetric states with energy eigenvalues  $E_i$  and eigenfunctions  $\psi_i$  of the 1-dimensional quantum-Hamiltonian

$$\hat{H} = -\frac{T^2}{2g} \sum_{\alpha=1}^n \sum_{j=1}^N \frac{\partial^2}{\partial x_{j,\alpha}^2} + \sum_{\alpha=1}^n \sum_{i<j} U(x_i - x_j) - \frac{\Delta}{2T} \sum_{\alpha,\beta=1}^n \sum_{i,j=1}^N \delta(x_{i,\alpha} - x_{j,\beta}). \quad (8)$$

From a classical statistical mechanics point of view, the operator  $\exp(-\hat{H}/T)$  is the transfer matrix corresponding to the partition function  $[Z_N^n]$ .

Using the representation of the density matrix in Eq. (7), we can perform the integrations in Eq. (6) easily. Taking the thermodynamic limit  $\beta_{qm} \sim L \rightarrow \infty$ , the free energy  $F_n$  of the replicated system is given by the ground state energy  $E_0$  of the quantum system in Eq. (8),

$$F_n = -T \ln[Z_N^n] = -TnN \ln(\mathcal{Z}_0) + E_0 L. \quad (9)$$

Therefore, the statistical properties of the line lattice in the thermodynamic limit  $L \rightarrow \infty$  are dominated by the ground state wave function  $\psi_0$ , which must be of bosonic symmetry [22]. To obtain the disorder averaged free energy  $[F]$  of the original line system within the replica method usually the identity  $[\ln Z_N] = \lim_{n \rightarrow 0} ([Z_N^n] - 1)/n$  is used. However, calculating the average  $[Z_N^n]$  for all values  $n > 0$  by analytic continuation of  $E_0(n)$  yields much additional information about the PDF of the free energy beyond  $[F]$ . Since  $[Z_N^n]$  is the characteristic function of the random variable  $[\ln Z]$ , expansion with respect to  $n$  shows that

$$nN \ln \mathcal{Z}_0 - \frac{E_0(n)L}{T} = \ln[Z_N^n] = \sum_{j=1}^{\infty} \frac{(-n)^j}{j!} \frac{[F^j]_c}{T^j}, \quad (10)$$

where  $[F^j]_c$  is the  $j$ th cumulant of the free energy. This identification relies on the possibility of an analytic expansion around  $n \rightarrow 0$ . That this is indeed the case for the line system considered here will be further discussed below.

Determining the PDF of the free energy is thus reduced to calculating the ground state energy of the quantum-mechanical system in Eq. (8). Before we can proceed with the calculation of  $E_0(n)$ , we have to specify the pair potential

---

<sup>4</sup> Here and in the following, we set  $k_B = 1$ .

$U(x)$ . We will consider the limit where the characteristic length scale of the short ranged pair potential goes to zero, leaving just a non-crossing condition for the lines. This replacement of the interaction potential by a pure geometric constraint for the line configurations does not change the physical mechanisms involved in the non-trivial characteristics of the line system. The crucial competition between the elasticity of single lines, the tendency of lines to follow energy valleys of the random potential, and the restriction of configurations by adjacent lines are preserved. Within the quantum-mechanical description of the lines, there is a convenient way to implement the non-crossing condition: As noted first by Pokrovsky and Talapov [14] for pure systems, the Pauli exclusion principle can be used to represent the elastic lines as world lines of fermions, which automatically avoids crossings. We thus look for a ground state wave function  $\psi_0$  with a suitable antisymmetry under particle permutations, which describes  $Nn$  particles with just an *attractive* interaction on contact between *any* two particles. It is interesting to note that we change the symmetry of the originally bosonic ground state function by hand by applying the exclusion principle. However, the ground state energy we are interested in is the same both in the fermion and the impenetrable boson description. Introducing the new subscript  $\mathbf{i} = (i - 1)n + \alpha$  instead of  $(i, \alpha)$  to number consecutively all  $nN$  particles, the Hamiltonian (8) can now be written as

$$\hat{H} = -\frac{\hbar^2}{2m} \sum_{\mathbf{i}=1}^{nN} \frac{\partial^2}{\partial x_{\mathbf{i}}^2} - 2c_0 \sum_{\mathbf{i}<\mathbf{j}} \delta(x_{\mathbf{i}} - x_{\mathbf{j}}), \quad (11)$$

with mass  $m = g$  and interaction amplitude  $c_0 = \Delta/2T$ . The explicit distinction between lines in the same or different replicas has disappeared from the Hamiltonian, but is hidden in the required transformation properties of the wave function under particle permutations. The appropriate symmetry of the ground state wave function is restricted by two conditions: (i)  $\psi_0$  must be *antisymmetric* if two of the  $N$  particles in the *same* replica (color) are interchanged (Fermi statistics). (ii)  $\psi_0$  must be *symmetric* if two of the  $n$  *different* replica (colored) particles corresponding to the same line are exchanged since replicas are equivalent. Due to its antisymmetry,  $\psi_0$  tends to zero if two particles of the same color approach each other and the attractive delta-function potential becomes inactive. This guarantees automatically that the impurity averaging results effectively in an attractive interaction on contact between particles of *different* color only. Therefore, the sum over pairs of lines interacting via a delta-function in Eq. (8) yields no contribution if  $\alpha = \beta$ , resulting in the sum over all pairs in Eq. (11). To conclude, the original quantum Hamiltonian (8) with  $U(x)$  replaced by the non-crossing condition for lines belonging to the same replica is equivalent to the Hamiltonian (11), if one solves for a ground state wave function of appropriate symmetry.

### 3 The Bethe Ansatz

In one dimension, a number of interacting quantum systems can be solved exactly by the Bethe ansatz [23,24]. Lieb and Liniger were the first to apply the Bethe ansatz method to a continuum quantum field theory by solving for the ground state energy and the excitation spectrum of the one dimensional interacting Bose gas with repulsive delta-function pair potentials [20]. While their Hamiltonian is exactly given by Eq. (11), the ground state wave function that we are looking for has a more complicated structure since it has to describe fermions of  $n$  different colors. The case  $n = 2$  corresponds to spin- $\frac{1}{2}$  fermions and was solved some time ago by Gaudin [25] for attractive interactions, and by Yang [18] for repulsive interactions. Choosing  $n = 3$  colors, we obtain a model for nuclear matter with an attractive quark-quark interaction, which has been discussed in connection with quantum chromodynamics and also studied by Bethe ansatz methods [26]. Since we are interested in an analytical continuation of the ground state energy for small  $n \ll 1$ , first we find a solution for integer  $n$  and then continue it analytically. According to the symmetry requirements discussed above, the allowed spatial wave functions of the  $U(n)$  fermions have to transform like the irreducible representation of the symmetric group  $\mathfrak{S}_{nN}$  corresponding to the Young diagram  $[n^N]$ , which consists of  $N$  rows of equal length  $n$ . Sutherland has constructed a general solution of the eigenvalue problem for Hamiltonian (11) with  $c_0 < 0$  when the wave function transforms like an arbitrary irreducible representation of the symmetric group [27]. The method involves a nested series of Bethe ansätze and leads to coupled integral equations for momentum densities. The same method has been applied later to the attractive case by Takahashi [19] and Kardar [8], leading to considerable simplifications in the solution of the Bethe ansatz equations. Before we turn to the interesting regime  $n \ll 1$ , we explain briefly the idea of the method of nested Bethe ansätze, in a simplified version for the relevant irreducible representation  $[n^N]$  with integer values  $n \geq 1$ .

#### 3.1 Bethe Ansatz equations for integer $n$

The eigenstates of the Hamiltonian (11) are given by Bethe's hypothesis [23]. For  $0 < x_{Q_1} < \dots < x_{Q_{nN}} < W$ , with  $W$  the transversal system size, we can write the wave function as

$$\Psi = \sum_{\mathcal{P}} [Q, P] \exp \left( i \sum_{j=1}^{nN} \lambda_{P_j} x_{Q_j} \right). \quad (12)$$

Here  $Q$  and  $P$  are permutations in  $\mathfrak{S}_{nN}$ , and the numbers  $[Q, P]$  form a  $(nN)! \times (nN)!$  matrix. In the following we denote the columns of this matrix

by the vector  $\xi_P = [\cdot, P]$ . Next, we define the permutation operators  $\mathcal{P}_{lm}$ , which act on the  $\xi_P$ . Their effect is to interchange the  $Q_l$  component with the  $Q_m$  component of the vector  $\xi_P$ , i.e.,  $\mathcal{P}_{lm}[Q, P] \equiv [Q', P]$  where the new permutation  $Q'$  is defined by  $Q'_l = Q_m$ ,  $Q'_m = Q_l$ , and  $Q'_j = Q_j$  for  $j \neq l, m$ . These operators form a  $(nN)!$  dimensional representation of the symmetric group  $\mathfrak{S}_{nN}$ . But this representation is reducible, i.e., for a wave function of a given symmetry, many coefficients  $[Q, P]$  are identical. Therefore, in the following we consider implicitly only the subspace of the original  $\xi_P$ -space which corresponds to the irreducible representation  $[n^N]$  of  $\mathfrak{S}_{nN}$ . On this subspace the operators  $\mathcal{P}_{lm}$  act as matrices of the dimension corresponding to the irreducible representation.

The requirement of a continuous wave function, which has cusps wherever two of its coordinates are equal in order to compensate the delta-function interaction in Eq. (11), imposes relations between the coefficients  $[Q, P]$ . In terms of two vectors  $\xi_P, \xi_{P'}$  corresponding to permutations  $P$  and  $P'$ , respectively, which differ by a transposition of  $i$  and  $j$ , i.e.,  $P_l = i = P'_m, P_m = j = P'_l$ , and  $P_j = P'_j$  for  $j \neq l, m$ , the relations can be written as

$$\xi_{P'} = Y_{ij}^{lm} \xi_P, \quad (13)$$

with the operator

$$Y_{ij}^{lm} = \frac{ic}{\lambda_i - \lambda_j - ic} + \frac{\lambda_i - \lambda_j}{\lambda_i - \lambda_j - ic} \mathcal{P}_{lm}, \quad (14)$$

and the rescaled interaction strength  $c = 2mc_0/\hbar^2 = g\Delta/T^3$ . If these relations are fulfilled, the wave function (12) is an eigenstate of the Hamiltonian (11) for *any* set of momenta  $\lambda_i$ . The allowed momenta are then restricted by imposing periodic boundary conditions on the wave function. Expressed in terms of  $\xi_I$  corresponding to the identity element  $I$  of  $\mathfrak{S}_{nN}$ , the conditions force  $\xi_I$  to be simultaneously an eigenvector of the  $nN$  matrix equations

$$e^{i\lambda_j W} \xi_I = X_{j+1j} X_{j+2j} \cdots X_{Nj} X_{1j} \cdots X_{j-1j} \xi_I, \quad (15)$$

with  $j = 1, \dots, nN$  and  $X_{ij}(\{\lambda_j\}) \equiv \mathcal{P}_{ij} Y_{ij}^{ij}$ . The  $\lambda_j$  which solve these equations depend, of course, on the chosen irreducible representation.

So far, we have considered only the spatial part (12) of the full fermionic wave function. The full wave function is given by the product of (12) and the color wave function  $\chi$ . The product has to be antisymmetric under simultaneous interchange of both position and color of two particles. To guaranty this property, the color wave function  $\chi$  has to transform like the conjugate irreducible representation  $[N^n]$ . One can think of the basis vectors of this representation as all the allowed color sequences of length  $nN$  which form by linear combination the function  $\chi$ . Now, the crucial point of Yang's and Sutherland's

method for determining the momenta  $\lambda_i$  is to solve the matrix equations in color space by regarding the color wave function as a spatial wave function describing  $(n-1)N$  distinguishable particles on a *discrete* cyclic chain with  $N$  identical vacancies. By making a generalized Bethe ansatz introduced by Yang, this new problem can be cast into matrix equations identical in form to the original one, but corresponding to the lower dimensional representation  $[N^{n-1}]$  for the color wave function  $\chi$ . This procedure is then continued until the problem has been reduced to one for particles of a single color only. To be more concrete, the periodic boundary conditions for  $\chi$  read

$$\mu_j \chi = X'_{j+1j} X'_{j+2j} \cdots X'_{Nj} X'_{1j} \cdots X'_{j-1j} \chi, \quad (16)$$

where

$$\mu_j = e^{i\lambda_j W}, \quad (17)$$

and  $X'_{ij}(\{\lambda_j\})$  is obtained from  $X_{ij}(\{\lambda_j\})$  by the replacement  $\mathcal{P}_{ij} \rightarrow -\mathcal{P}_{ij}$ . This change of sign for the permutation operator comes from the fact that in general two representation matrices of a permutation  $P$  corresponding to the original and conjugated representation, respectively, differ by the parity of  $P$  only. To solve Eqs. (16) we use the generalized Bethe hypothesis of Yang for  $\chi$  on the discrete cyclic chain. It consists in the ansatz

$$\chi = \sum_P [Q, P] G(\lambda_{P_1}^{(2)}, y_{Q_1}) \cdots G(\lambda_{P_{(n-1)N}}^{(2)}, y_{Q_{(n-1)N}}), \quad (18)$$

where the integers  $1 \leq y_{Q_1} < \dots < y_{Q_{(n-1)N}} \leq nN$  denote the coordinates of the distinguishable particles, and  $\lambda_1^{(2)}, \dots, \lambda_{(n-1)N}^{(2)}$  is a set of unequal complex quasi-momenta.  $P$  and  $Q$  are now elements of  $\mathfrak{S}_{(n-1)N}$ . The coefficients  $[Q, P]$  form now a  $(n-1)N \times (n-1)N$  matrix, the columns of which we denote by  $\xi'_P$ . Again, we define permutation operators  $\hat{\mathcal{P}}_{lm}$  that act on  $\xi'_P$  so that they interchange  $Q_l$  and  $Q_m$ . By considering a suitable subspace of the  $\xi'_P$ -space, these operators are chosen to form the irreducible representation  $[N^{n-1}]$  of  $\mathfrak{S}_{(n-1)N}$ , in order to assure that the color wave function has the appropriate symmetry. Physically, the number  $\chi$  associated with a particular set  $\{y_1, \dots, y_{(n-1)N}\}$  and permutation  $Q$  can be interpreted as the amplitude for finding a particular arrangement of colors for the  $nN$  particles. Indeed, the positions of all the particles of one color, say red, determine the  $y_i$  of the remaining particles, and the color arrangement of these remaining  $(n-1)N$  particles can be identified with the permutation  $Q$ . To complete the ansatz, we have to specify the function  $G(\lambda, y)$ ,

$$G(\lambda, y) = \prod_{j=1}^{y-1} \frac{i(\lambda_j - \lambda) + c/2}{i(\lambda_{j+1} - \lambda) - c/2}. \quad (19)$$

The requirement that this ansatz for  $\chi$  is a simultaneous eigenvector of the  $nN$  matrix equations (16) imposes relations between the  $\xi'_P$ , as the original

eigenvalue problem for the Hamiltonian (11) does for the  $\xi_P$ . These relations can again be written as

$$\xi'_{P'} = Y'^{ij}_{lm} \xi'_P, \quad (20)$$

with the operator

$$Y'^{ij}_{lm} = \frac{-ic}{\lambda_i^{(2)} - \lambda_j^{(2)} + ic} + \frac{\lambda_i^{(2)} - \lambda_j^{(2)}}{\lambda_i^{(2)} - \lambda_j^{(2)} + ic} \hat{\mathcal{P}}_{lm}, \quad (21)$$

and  $P, P'$  defined as above Eq. (13). Finally, we have to impose periodic boundary conditions on  $\chi$ . Using the relations (20), we obtain for the vector  $\xi'_I$  the  $(n-1)N$  matrix equations

$$\prod_{j=1}^{nN} \frac{i(\lambda_l^{(2)} - \lambda_j) - c/2}{i(\lambda_l^{(2)} - \lambda_j) + c/2} \xi'_I = X''_{l+1l} \cdots X''_{(n-1)Nl} X''_{1l} \cdots X''_{l-1l} \xi'_I, \quad (22)$$

for  $l = 1, \dots, (n-1)N$ , and with

$$X''_{ij}(\{\lambda_l^{(2)}\}) \equiv \hat{\mathcal{P}}_{ij} Y'^{ij}_{ij} = \frac{\lambda_i^{(2)} - \lambda_j^{(2)} - ic}{\lambda_i^{(2)} - \lambda_j^{(2)} + ic} X'_{ij}(\{\lambda_l^{(2)}\}). \quad (23)$$

Substituting Eq. (23) in Eq. (22), we obtain new matrix equations, which parallel in form precisely the original equations (16) for the color wave function, but with operators  $X'_{ij}$ , in which the quasi-momenta  $\lambda_l^{(2)}$  have replaced the original momenta  $\lambda_l$ . The new equations read

$$\mu'_I \xi'_I = X'_{l+1l} \cdots X'_{(n-1)Nl} X'_{1l} \cdots X'_{l-1l} \xi'_I, \quad (24)$$

with the new set of  $\mu'_I$  defined via

$$-\mu'_I \prod_{m=1}^{(n-1)N} \frac{i(\lambda_l^{(2)} - \lambda_m^{(2)}) - c}{i(\lambda_l^{(2)} - \lambda_m^{(2)}) + c} = \prod_{j=1}^{nN} \frac{i(\lambda_l^{(2)} - \lambda_j) - c/2}{i(\lambda_l^{(2)} - \lambda_j) + c/2}. \quad (25)$$

Thus Eq. (16) is reduced to the lower dimensional Eq. (24), and the eigenvalue  $\mu_j$  in Eq. (17), which is obtained from the ansatz (18), is

$$\mu_j = \prod_{m=1}^{(n-1)N} \frac{i(\lambda_j - \lambda_m^{(2)}) + c/2}{i(\lambda_j - \lambda_m^{(2)}) - c/2}. \quad (26)$$

To reduce Eq. (24) further and to determine the eigenvalue  $\mu'_I$ , we apply the procedure described above again in the representation  $[N^{n-2}]$ , introducing the quasi-momenta  $\lambda_j^{(3)}$ . This process terminates after  $n-1$  iterations and yields Sutherland's Bethe ansatz equations for the  $Nn(n+1)/2$  complex momenta  $\lambda_i^{(\alpha)}$ , with  $\alpha = 1, \dots, n$  and  $i = 1, \dots, (n+1-\alpha)N$ . Here we have denoted the original momenta  $\lambda_j$  by  $\lambda_j^{(1)}$ .

Comparing Eq. (17) with Eq. (26), we obtain

$$e^{i\lambda_i^{(1)}W} = \prod_{j=1}^{(n-1)N} \frac{i(\lambda_i^{(1)} - \lambda_j^{(2)}) + c/2}{i(\lambda_i^{(1)} - \lambda_j^{(2)}) - c/2}, \quad \text{with } (\mathbf{i} = 1, \dots, nN). \quad (27)$$

Continuing the iteration, we obtain from Eq. (25) with  $\mu'_i$  given by Eq. (26), with  $\lambda_j$  and  $\lambda_m^{(2)}$  replaced by corresponding higher order quasi-momenta, the set of equations

$$\begin{aligned} \prod_{j=1}^{mN} \frac{i(\lambda_i^{(n-m+2)} - \lambda_j^{(n-m+1)}) - c/2}{i(\lambda_i^{(n-m+2)} - \lambda_j^{(n-m+1)}) + c/2} &= - \prod_{l=1}^{(m-1)N} \frac{i(\lambda_i^{(n-m+2)} - \lambda_l^{(n-m+2)}) - c}{i(\lambda_i^{(n-m+2)} - \lambda_l^{(n-m+2)}) + c} \\ &\times \prod_{\mathbf{p}=1}^{(m-2)N} \frac{i(\lambda_i^{(n-m+2)} - \lambda_{\mathbf{p}}^{(n-m+3)}) + c/2}{i(\lambda_i^{(n-m+2)} - \lambda_{\mathbf{p}}^{(n-m+3)}) - c/2}, \quad \text{with } \begin{pmatrix} \mathbf{i} = 1, \dots, (m-1)N \\ m = n, \dots, 3 \end{pmatrix}. \end{aligned} \quad (28)$$

Finally, the iteration ends at the representation  $[N]$ , which corresponds to  $X'_{ij} = 1$  in Eq. (24). Therefore, this equation is trivially fulfilled with  $\mu'_i = 1$ , corresponding together with Eq. (25) to

$$\prod_{j=1}^{2N} \frac{i(\lambda_i^{(n)} - \lambda_j^{(n-1)}) - c/2}{i(\lambda_i^{(n)} - \lambda_j^{(n-1)}) + c/2} = - \prod_{l=1}^N \frac{i(\lambda_i^{(n)} - \lambda_l^{(n)}) - c}{i(\lambda_i^{(n)} - \lambda_l^{(n)}) + c}, \quad \text{with } (\mathbf{i} = 1, \dots, N). \quad (29)$$

In the following, we will make a simple ansatz [19,8] for the complex momenta  $\lambda_i^{(\alpha)}$ , which solve Eqs. (27)-(29) in the limit  $W \rightarrow \infty$ , leaving only one set of  $N$  independent equations for the  $N$  different real parts of the original momenta  $\lambda_i \equiv \lambda_i^{(1)}$ . To motivate this ansatz, we consider for the time being the case of a single line ( $N = 1$ ) coming in  $n$  colors. This corresponds to the representation  $[n]$  for  $n$  bosons without spin. Under the attractive interaction they form a bound cluster, which is described by complex momenta  $\lambda_\alpha = ic(n+1-2\alpha)/2$  ( $\alpha = 1, \dots, n$ ) forming a so-called “ $n$  string” [24]. Switching back to the general case of  $N$  lines, but now for vanishing disorder strength  $\Delta$  so that  $c = 0$ , the problem becomes that of  $N$  free fermions without spin ( $n = 1$ ) represented by the Young diagram  $[1^N]$ . In this case, the momenta are equally spaced along the real axis between  $-k_F$  and  $k_F = \pi\rho$ , where  $\rho = N/W$  is the density of particles. With this two limiting cases in mind, it is reasonable to make the general ansatz for large  $W$

$$\lambda_j^{(n)} = k_j + iB_{j,1}^{(n)} \quad (j = 1, \dots, N), \quad (30)$$

$$\lambda_{\mathbf{i}=(j-1)(m+1)+\alpha}^{(n-m)} = k_j + ic \left( 1 - \alpha + \frac{m}{2} \right) + iB_{j,\alpha}^{(n-m)} \quad (31)$$

$$(j = 1, \dots, N; \alpha = 1, \dots, m+1; m = 1, \dots, n-2),$$

$$\lambda_{\mathbf{i}=(j-1)n+\alpha}^{(1)} = k_j + ic \left( 1 - \alpha + \frac{n-1}{2} \right) + iB_{j,\alpha}^{(1)} \quad (32)$$

$$(j = 1, \dots, N; \alpha = 1, \dots, n),$$

where the  $k_j$  are *real* valued momenta and the correction terms  $B_{j,\alpha}^{(n-m)}$  will be proven to vanish in the limit  $W \rightarrow \infty$  below. In constructing this ansatz we start with the quasi-momenta  $\lambda_i^{(n)}$ , which were introduced in the last iteration step of the nested Bethe ansatz. In this last step the original problem of  $nN$  interacting particles was completely reduced to that of  $N$  colorless cluster fermions. Therefore, in analogy to the usual fermionic case discussed above, we make the ansatz that the quasi-momenta  $\lambda_i^{(n)}$  correspond to the real valued cluster momenta  $k_j$ . But due to the complex structure of the effective cluster-cluster interaction, the momenta  $k_j$  are, of course, no longer homogeneously distributed. To get a physical picture of the internal structure of a single cluster of fermions, we think of it as an “ $n$  string” composed of  $n$  bosons which are hold together by the attractive interaction. From the above discussion of the  $N = 1$  case we know that the “internal” boson momenta of the cluster are equally spaced along the imaginary axis. Therefore, the single cluster wave function is localized in space within a range of size  $1/c = T^3/g\Delta$ . The ansätze (30)-(32) show that also for a finite cluster density in the limit  $W \rightarrow \infty$ , the overlap of clusters can be neglected, particularly with regard to the internal structure of the clusters. Thus each cluster’s momenta are simply given by the momenta of an unperturbed “ $n$  string” plus the collective real valued cluster momentum  $k_j$ . This leads to the  $nN$  original momenta  $\lambda_i^{(1)}$  of Eq. (32). The intermediate quasi-momenta of Eq. (31) can be understood as that of smaller sub-clusters which appear during the iterative scheme of the nested Bethe ansätze.

We now prove that the ansätze (30)-(32) indeed solve Eqs. (27)-(29) in the limit  $W \rightarrow \infty$ , leaving a new set of only  $N$  equations to determine the  $k_j$ ’s. In substituting the ansatz in Eqs. (27)-(29) we keep the correction terms  $B_{j,\alpha}^{(n-m)}$  only in factors which would become zero otherwise. The resulting equations for the correction terms have two important properties: (i) From the first set of  $nN$  equations [Eq. (27)] one observes that the  $B_{j,\alpha}^{(n-m)}$  have to vanish exponentially fast if  $W \rightarrow \infty$ . (ii) The solutions depend formally on the real momenta  $k_j$ , which are still free parameters. In the following we will show that these  $k_j$  have to fulfill necessarily  $N$  independent equations in order to make the equations for the  $B_{j,\alpha}^{(n-m)}$  consistent and thus solvable.

Multiplying the  $n$  equations of Eq. (27) with the ansatz substituted and  $\mathbf{i} =$

$(i-1)n + \alpha$  with  $i$  fixed and  $\alpha = 1, \dots, n$ , we obtain

$$e^{ik_i n W} = (-1)^{n-1} \prod_{\beta=1}^{n-1} \frac{B_{i,\beta}^{(1)} - B_{i,\beta}^{(2)}}{B_{i,\beta+1}^{(1)} - B_{i,\beta}^{(2)}} \prod_{j=1}^N \prod_{\substack{\alpha=1 \\ j \neq i}}^{n-1} \frac{i(k_i - k_j) + \alpha c}{i(k_i - k_j) - \alpha c}. \quad (33)$$

In the next step we eliminate all correction terms  $B_{i,\alpha}^{(1)}, B_{i,\alpha}^{(2)}$  from this equation without calculating them explicitly. Thus we substitute the ansatz into the set of Eqs. (28). The cluster momenta  $k_j$  drop out and we get for  $m = 3, \dots, n$ ;  $i = 1, \dots, N$ , and  $\beta = 2, \dots, m-2$ , the new set of equations

$$-\frac{B_{i,\beta}^{(n-m+2)} - B_{i,\beta}^{(n-m+1)}}{B_{i,\beta}^{(n-m+2)} - B_{i,\beta+1}^{(n-m+1)}} = \frac{B_{i,\beta}^{(n-m+2)} - B_{i,\beta-1}^{(n-m+2)}}{B_{i,\beta}^{(n-m+2)} - B_{i,\beta+1}^{(n-m+2)}} \cdot \frac{B_{i,\beta}^{(n-m+2)} - B_{i,\beta}^{(n-m+3)}}{B_{i,\beta}^{(n-m+2)} - B_{i,\beta-1}^{(n-m+3)}}. \quad (34)$$

In the special case  $\beta = 1$  we have

$$-\frac{B_{i,1}^{(n-m+2)} - B_{i,1}^{(n-m+1)}}{B_{i,1}^{(n-m+2)} - B_{i,2}^{(n-m+1)}} = \frac{B_{i,1}^{(n-m+2)} - B_{i,1}^{(n-m+3)}}{B_{i,1}^{(n-m+2)} - B_{i,2}^{(n-m+2)}}, \quad (35)$$

and similarly for  $\beta = m-1$ ,

$$-\frac{B_{i,m-1}^{(n-m+2)} - B_{i,m-1}^{(n-m+1)}}{B_{i,m-1}^{(n-m+2)} - B_{i,m}^{(n-m+1)}} = \frac{B_{i,m-1}^{(n-m+2)} - B_{i,m-2}^{(n-m+2)}}{B_{i,m-1}^{(n-m+2)} - B_{i,m-2}^{(n-m+3)}}. \quad (36)$$

Now we take for fixed  $m \in \{3, \dots, n\}$  and  $i \in \{1, \dots, N\}$  the product of the  $m-1$  Eqs. (34)-(36). Introducing the following ratio of correction terms,

$$\mathcal{B}_i(m) = \prod_{\beta=1}^{m-1} \frac{B_{i,\beta}^{(n-m+2)} - B_{i,\beta}^{(n-m+1)}}{B_{i,\beta}^{(n-m+2)} - B_{i,\beta+1}^{(n-m+1)}}, \quad (37)$$

we obtain the simple recursion relation

$$\mathcal{B}_i(m) = -\mathcal{B}_i(m-1). \quad (38)$$

From the definition of  $\mathcal{B}_i(m)$  it is easy to realize that the coefficient of the right hand side of Eq. (33) is given by  $(-1)^{n-1} \mathcal{B}_i(n) = -\mathcal{B}_i(2)$ . Finally, to obtain  $\mathcal{B}_i(2)$  we substitute the ansätze of Eqs. (30)-(32) into Eq. (29) keeping again the correction terms only in factors which would become zero otherwise. For  $i = 1, \dots, N$ , we thus obtain

$$\mathcal{B}_i(2) = \frac{B_{i,1}^{(n)} - B_{i,1}^{(n-1)}}{B_{i,1}^{(n)} - B_{i,2}^{(n-1)}} = -1. \quad (39)$$

This result shows that the correction terms dependent coefficient of Eq. (33) has to be one in order to have a consistent set of equations for the  $B_{j,\alpha}^{(n-m)}$ .

This in turn determines the allowed real parts  $k_j$  of the original momenta  $\lambda_i \equiv \lambda_i^{(1)}$ . They have to fulfill Eq. (33), which now reads

$$e^{ink_j W} = \prod_{\substack{l=1 \\ l \neq j}}^N \prod_{\alpha=1}^{n-1} \frac{i(k_j - k_l)/c + \alpha}{i(k_j - k_l)/c - \alpha} \quad (j = 1, \dots, N). \quad (40)$$

These are the final Bethe Ansatz equations<sup>5</sup> which have to be solved to obtain the ground state energy of the quantum Hamiltonian  $\hat{H}$  in Eq. (11) in the thermodynamic limit, as

$$E_0 = \frac{\hbar^2}{2m} \sum_{i=1}^{nN} \lambda_i^2 = \frac{\hbar^2 c^2}{24m} n(1 - n^2)N + \frac{n\hbar^2}{2m} \sum_{j=1}^N k_j^2. \quad (41)$$

In the last equation, we have used Eq. (32). The Bethe ansatz Eq. (40) has been analyzed in Ref. [8] to obtain the free energy of the line lattice to leading order in the density  $\rho = N/W$ . The central result of this reference is an integral equation for integer  $n$ , which was obtained from Eq. (40) in the limit  $W, N \rightarrow \infty$  with  $\rho$  fixed, by using the fact that  $[W(k_{j+1} - k_j)]^{-1}$  becomes a continuous function in that limit. By taking the limit  $n \rightarrow 0$ , and subsequently the limit  $\rho \rightarrow 0$ , the kernel of the integral equation becomes of Hilbert type, thus enabling an analytic solution [28]. To obtain the probability distribution function of the free energy, we have to determine the ground state energy as a function of  $n$  for small but finite arguments. Since extracting this information by an exact method from the integer  $n$  integral equation of Ref. [8] is not obvious, here we start with a direct analytical continuation of the Bethe ansatz Eq. (40) to non-integer  $n$ .

### 3.2 Analytic continuation in $n$

In what follows, we show how to evaluate the right hand side (rhs) of Eq. (40) for non-integer values of  $n$ . The product over the replica index  $\alpha$  represents simply the extension of a factorial to complex numbers. Therefore, we can make use of the recursion relation for the complex gamma function,  $\Gamma(z+1) = z\Gamma(z)$ , to obtain for real valued  $k$  the relation

---

<sup>5</sup> The same equations have been obtained for the case  $n = 3$  in the context of quantum chromodynamics [26] by a more direct approach which does not use Sutherland's nested series of Bethe ansätze. Instead it was a priori assumed that the overlap of clusters can be neglected in calculating the momenta in the thermodynamic limit.

$$\begin{aligned}
\prod_{\alpha=1}^{n-1} \frac{ik/c + \alpha}{ik/c - \alpha} &= (-1)^{n-1} \frac{\Gamma(1 - ik/c)\Gamma(n + ik/c)}{\Gamma(1 + ik/c)\Gamma(n - ik/c)} \\
&= (-1)^n \frac{\Gamma(-ik/c)\Gamma(n + ik/c)}{\Gamma(ik/c)\Gamma(n - ik/c)}, \tag{42}
\end{aligned}$$

which is well defined for all  $n$ . Using this representation of the finite product, and taking the logarithm of both sides of Eq. (40), the proper extension of the Bethe ansatz equations to real valued  $n$  reads

$$nk_j W = -i \sum_{\substack{l=1 \\ l \neq j}}^N \ln \left[ \frac{\Gamma(n + i(k_j - k_l)/c)\Gamma(-i(k_j - k_l)/c)}{\Gamma(n - i(k_j - k_l)/c)\Gamma(i(k_j - k_l)/c)} \right], \tag{43}$$

where some care has to be taken to conserve the property that the ground state has a total momentum of zero, i.e.,  $\sum_{j=1}^N k_j = 0$ . To express the argument of the logarithm in terms of more elementary functions, we rewrite it as the infinite product

$$\frac{\Gamma(n + ik/c)\Gamma(-ik/c)}{\Gamma(n - ik/c)\Gamma(ik/c)} = \prod_{m=0}^{\infty} \frac{m^2 + nm + (k/c)^2 + ink/c}{m^2 + nm + (k/c)^2 - ink/c}. \tag{44}$$

Here we have used the product representation  $1/\Gamma(z) = ze^{\gamma z} \prod_{m=1}^{\infty} (1+z/m)e^{-z/m}$  of the gamma function with  $\gamma$  the Euler constant [29]. Next we write the last expression as a product of exponential factors to compensate the logarithm in Eq. (43). Using  $\arctan(z) = \frac{1}{2i} \ln((1+iz)/(1-iz))$  we obtain

$$\frac{\Gamma(n + ik/c)\Gamma(-ik/c)}{\Gamma(n - ik/c)\Gamma(ik/c)} = \prod_{m=0}^{\infty} \exp \left[ 2i \arctan \left( \frac{nk/c}{m^2 + nm + (k/c)^2} \right) \right]. \tag{45}$$

This result shows that the rhs of Eq. (43) is indeed a real valued expression, and the final Bethe ansatz equation for arbitrary real  $n$  becomes

$$nk_j W = \sum_{\substack{l=1 \\ l \neq j}}^N g_n \left( \frac{k_j - k_l}{c} \right), \tag{46}$$

with the function

$$g_n(x) = 2 \sum_{m=0}^{\infty} \arctan \left( \frac{nx}{m^2 + nm + x^2} \right). \tag{47}$$

This is the central result of this section. The function  $g_n(x)$  has no poles for real valued  $x$ , is bounded between  $\pm\pi$  and converges to  $\pm n\pi$  for  $x \rightarrow \pm\infty$ , see Fig. 1. Notice that the jump of  $2\pi$  at  $x = 0$  is produced solely by the  $m = 0$  term in Eq. (47), whereas the remaining terms are continuous.

This Bethe ansatz equation is valid for all  $n$  and for all line densities  $\rho$ . To compare it with results already existing in literature we consider two limiting

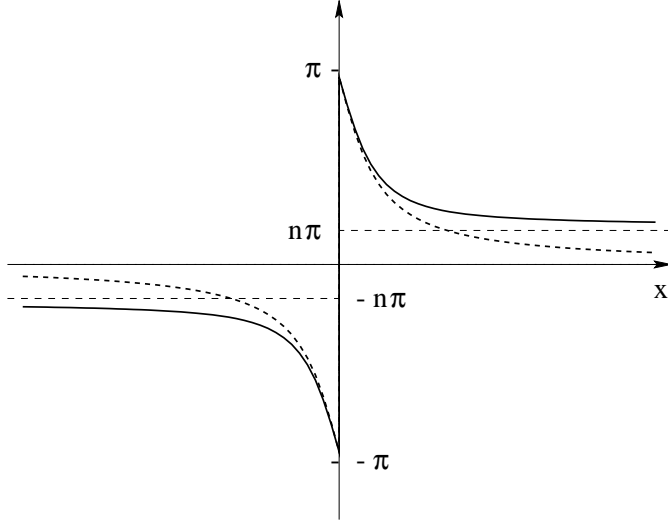


Fig. 1. Both the function  $g_n(x)$  (solid curve) and its limiting form  $2 \arctan(n/x) = \pi \operatorname{sgn}(x) - 2 \arctan(x/n)$  (dashed curve) for  $x \ll 1$ ,  $n \ll 1$  show a jump of  $2\pi$  at  $x = 0$ .

cases. For  $n = 1$  we have  $g_n(x) = \pi \operatorname{sgn}(x)$ , where  $\operatorname{sgn}(x)$  is the sign function. The solution of Eq. (46) then simply consists of momenta  $k_j$  which are equally spaced between  $-\pi\rho$  and  $\pi\rho$  for  $W, N \rightarrow \infty$ . This is the free fermion situation corresponding to lines which wander due to thermal fluctuations only. Notice that with only one color of lines ( $n = 1$ ) present, the disorder induced inter-color interaction is, of course, inactive. The same situation is expected to appear in the zero disorder limit  $c \rightarrow 0$ . Indeed, in this limit  $g_n(x \sim 1/c \rightarrow \infty) \rightarrow n\pi \operatorname{sgn}(x)$  and the  $n$ 's on both sides of Eq. (46) cancel, leading again to the free fermion result. The solution of Eq. (46) in the limit  $n \rightarrow 0$  gives the disorder averaged free energy of lines in a random environment following Eqs. (10) and (41). Expanding  $g_n(x)$  to first order in  $n$ , we get from Eq. (46)

$$k_j W = \sum_{\substack{l=1 \\ l \neq j}}^N \left[ \frac{c}{k_j - k_l} + \pi \coth \left( \frac{\pi(k_j - k_l)}{c} \right) \right], \quad (48)$$

where we have used the representation  $\pi \coth(\pi x) = 1/x + 2x \sum_{m=1}^{\infty} (m^2 + x^2)^{-1}$  of the hyperbolic cotangent. It is easily seen that this equation corresponds to the discrete momenta version of the integral equation derived by a different technique for treating the  $n \rightarrow 0$  limit in Ref. [8]. In this reference the corresponding integral equation is solved in the dilute limit  $\rho/c \rightarrow 0$  yielding a free energy with steric interaction between lines proportional to  $\rho^2$  (instead of the behavior  $\sim \rho^3$  due to thermal fluctuations). From Eq. (48), the free energy can be obtained at *all* densities [30].

Now consider the thermodynamic limit  $N, W \rightarrow \infty$  of Eq. (46), while keeping the density  $\rho = W/N$  fixed. The employed technique is analogous to that of Lieb and Liniger [20], using the fact that the function  $\varrho(k_j) = [W(k_{j+1} - k_j)]^{-1}$

becomes continuous in this limit. The limiting behavior gives the density of states in the sense that  $W \varrho(k) dk =$  number of allowed  $k$ -values in the interval  $[k, k+dk]$ . For a given density  $\rho$ , the boundary (Fermi) momentum  $K \equiv k_N = -k_1$  is determined by the condition

$$\int_{-K}^K \varrho(k) dk = \rho, \quad (49)$$

while the ground state energy is given by

$$E_0 = \frac{\hbar^2 c^2}{24m} n(1-n^2) \rho W + \frac{\hbar^2 n W}{2m} \int_{-K}^K k^2 \varrho(k) dk. \quad (50)$$

Calculating the differences of Eq. (46) between all adjacent momenta  $k_{j+1}$  and  $k_j$  and expanding with respect to the difference  $k_{j+1} - k_j$ , yields an integral equation for  $\varrho(k)$ ,

$$nk = \int_{-K}^K g_n \left( \frac{k - k'}{c} \right) \varrho(k') dk', \quad (51)$$

for all  $k \in [-K, K]$ . This integral equation is not amenable to a closed form solution because of the complicated form of its kernel  $g_n(x)$ . However, the kernel is non-singular, and thus a numerical treatment seems feasible, which we leave for a future publication [30]. Instead, in the next Section we will show that taking the limit of small  $\rho/c$  leads to an interesting simplification which paves the way for a description of the replicated lines in terms of a pure, weakly interacting Bose gas.

## 4 Mapping to a weakly repulsive Bose gas

In this section, we develop a novel mapping of the dilute disordered line lattice onto a weakly interacting pure Bose gas. This mapping then provides a valuable tool to obtain exact results for the probability distribution of the free energy in the important limits of low density  $\rho$  or high disorder strength  $\Delta \sim c$ . This is the relevant limit for the critical behavior at the transition to a line-free system, e.g., for flux lines expelled at  $H_{c1}$  from superconductors or for domain walls at the commensurate-incommensurate transitions in absorbed layers or charge density waves.

From Eq. (49) one observes that the cutoff momentum  $K$  goes to zero in the limit of  $\rho \rightarrow 0$ . Therefore the behavior of  $g_n(x)$  for  $x \ll 1$  determines the solution of the integral Eq. (51) in the limit  $\rho/c \ll 1$ . This limit has to be analyzed very carefully since we have to keep the  $n$  dependence of  $g_n(x)$  to all orders to obtain a complete expansion of the ground state energy  $E_0$  in  $n$ ,

which is exact to first order in  $\rho/c \ll 1$ . Expressing the arctan of the  $m = 0$  part of Eq. (47) in terms of its inverse argument, and expanding the remaining terms in  $x$ , we obtain

$$g_n(x) = \pi \operatorname{sgn}(x) - 2 \arctan\left(\frac{x}{n}\right) + x \sum_{m=1}^{\infty} \frac{2n}{m(m+n)} + \mathcal{O}(x^3). \quad (52)$$

Note that we are interested in an expansion of the ground state energy  $E_0$  around  $n = 0$ . Independent on how small the ratio  $\rho/c$  and therefore the argument of  $g_n(x)$  is, the final expansion in  $n$  for fixed  $\rho/c$  tests arbitrarily small values of  $n$  and thus can render the  $\arctan(x/n)$  in Eq. (52) of order one. Therefore, an expansion of this term is not justified. In contrast, the remaining terms with  $m \geq 1$  in Eq. (52) tend always to zero for both  $x \ll 1$  and  $n \ll 1$  and can be safely neglected. Thus, retaining the first two terms of Eq. (52) only [see Fig. 1] and taking the derivative of Eq. (51) with respect to  $k$ , we obtain the integral equation

$$\int_{-K}^K \frac{2nc}{(nc)^2 + (k - k')^2} \varrho(k') dk' = 2\pi\varrho(k) - n, \quad (53)$$

which yields the complete  $n$  dependence of  $\varrho(k)$  to first order in  $\rho/c$  exactly. The crucial observation is that this equation is identical to that obtained by Lieb and Liniger for their exact Bethe ansatz solution of the one-dimensional Bose gas with repulsive delta-function interactions [20].

To obtain a physical understanding of the relation between the replicated line lattice and the Bose gas, we change variables as follows: Define the function  $\varrho_b(k) = \varrho(k/n)/n$ , the cutoff momentum  $K_b = nK$ , the mass  $m_b = nm$  and the rescaled interaction strength  $c_b = n^2c$ . With this new variables Eqs. (53), (49) read

$$\int_{-K_b}^{K_b} \frac{2c_b}{c_b^2 + (k - k')^2} \varrho_b(k') dk' = 2\pi\varrho_b(k) - 1, \quad \int_{-K_b}^{K_b} \varrho_b(k) dk = \rho. \quad (54)$$

The bosonic ground state energy, i.e., the second term of Eq. (50) becomes

$$E_{0,b} = \frac{\hbar^2 W}{2m_b} \int_{-K_b}^{K_b} k^2 \varrho_b(k) dk. \quad (55)$$

These equations represent the exact ground state (with energy  $E_{0,b}$ ) of a Bose gas with *repulsive* interactions, described by the Hamiltonian

$$\hat{H}_b = -\frac{\hbar^2}{2m_b} \sum_{i=1}^N \frac{\partial^2}{\partial x_i^2} + 2c_{0,b} \sum_{i<j} \delta(x_i - x_j), \quad (56)$$

for  $N \rightarrow \infty$  with fixed density  $\rho$  of bosons [20]. Due to the definition of  $c = 2mc_0/\hbar^2$  the amplitude of the interaction is given by  $c_{0,b} = nc_0$ . The correspondence can be summarized as follows: The exact ground state solution of

the quantum Hamiltonian in Eq. (11) for *attracting* particles, each appearing in  $n$  colors, is in the dilute limit  $\rho/c \ll 1$ , and to all orders in  $n$  around  $n = 0$ , the same as the ground state solution of the Bose gas Hamiltonian of Eq. (56) with *repulsive* interactions. For comparison with the usual mapping between elastic lines and world lines of bosons for pure systems, both the correspondence of parameters for the pure case and the novel analogy of quantities in the random system are summarized in Tables 1 and 2.

Table 1

The usual correspondence of the parameters of a  $d - 1$ -dimensional Bose gas and a  $d$ -dimensional lattice of lines without a random potential. The interaction potential between vortex lines maps to the Boson pair potential. In  $d = 2$  dimensions, non-crossing lines are modeled by hard core bosons or, equivalently, free fermions.

model	mass	Planck's constant	inverse temperature
Bose gas	$m_b$	$\hbar$	$\hbar/\beta_{\text{qm}}$
non-random lines	$g$	$T$	$L$

Table 2

The correspondence of parameters in the novel analogy between the one-dimensional Bose gas and the two-dimensional replica theory of lines. The density of bosons and (non-replicated) lines, respectively, is in both descriptions given by  $\rho$ .

model	mass	Planck's constant	inverse temperature	contact interaction	effective interaction
Bose gas	$m_b$	$\hbar$	$\hbar/\beta_{\text{qm}}$	$c_{0,b}$ (repulsive)	$c_b$ $\equiv 2m_b c_{0,b}/\hbar^2$
replicated lines	$nm$ $\equiv ng$	$T$	$L$	$nc_0 \equiv n\Delta/2T$ (attractive)	$n^2c$ $\equiv n^2g\Delta/T^3$

The correspondence between the Bose gas and the replica theory of lines can be interpreted physically as follows: As we have seen in Section 3.1, the Bethe ansatz solution can be interpreted as  $n$  lines of different colors forming a cluster due to the pair attraction of amplitude  $c_0$ . This suggests considering these clusters as new particles of mass  $nm = ng$ , then appearing as the components of the Bose gas described by Eq. (56). To obtain insight in the effective strength of the contact interaction between these composite bosons, consider two clusters, each composed of  $n$  lines of different colors. Since particles of the same color avoid each other like free fermions or, equivalently, bosons with hard core repulsion, some inter-cluster interactions are “screened,” see Fig. 2. There are  $n!$  orderings of particles within a cluster, each ordering providing the same number of pair interactions given by  $1 + \dots + (n - 1) = \frac{1}{2}n(n - 1)$

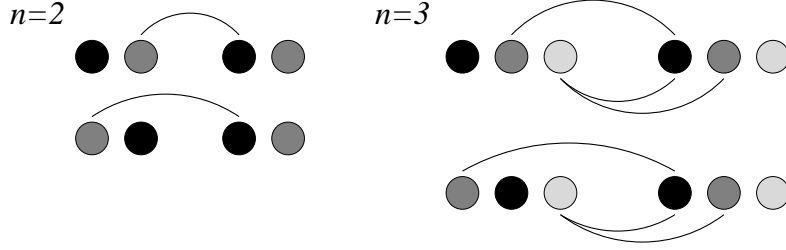


Fig. 2. The origin of the effective cluster-cluster interaction: For  $n = 2$  there is for both configurations only one inter-cluster interaction possible since the black particle of the first cluster is blocked by the black particle of the second cluster from interacting with the dark gray particle. For  $n = 3$  only two typical configurations are shown. It is easy to convince oneself that each of the  $3!$  configurations allows for three interactions suggesting  $1 + \dots + (n - 1) = \frac{1}{2}n(n - 1)$  pair interactions for  $n$ -particle clusters.

due to screening. Finally, we have to take into account that in the quantum Hamiltonian (11), which corresponds to the replica theory of lines, the interaction sum runs implicitly for two given clusters over all different colors  $\alpha \neq \beta$  instead of running over color pairs  $\alpha < \beta$  only. Therefore, the total amplitude of the contact interaction between two clusters is given by  $n(n - 1)c_0$ , which yields a repulsion of amplitude  $-nc_0$  in the limit  $n \ll 1$ , in agreement with our findings (see Table 2). That this naive estimate produces the correct result to first order in  $\rho/c$  is presumably related to the fact that the internal structure of the clusters does not matter in the dilute limit since the distance between clusters is much larger than cluster size  $\sim 1/c$ .

Having established the analogy between the replica theory of lines and the Bose gas, one can take advantage of the many results for the one-dimensional Bose gas accumulated during the past decades [20,31–33]. In the following, we focus on the ground state energy  $E_{0,b}$  as given by Eq. (55) to obtain the free energy  $F_n$  of the replicated line system using Eq. (9). The only dimensionless intensive variable in the Bose gas problem is  $\gamma = c_b/\rho = n^2 g\Delta/\rho T^3$ . Thus the ground state energy can be written as

$$E_{0,b} = \frac{\hbar^2}{2m_b} W \rho^3 e(\gamma), \quad (57)$$

where  $e(\gamma)$  is a dimensionless monotonically increasing function of  $\gamma$  [20]. Since we are interested in the limit  $n \ll 1$ , we have to consider the weak coupling limit of the Bose gas. In the limit  $c_b \rightarrow 0$ , the integral equation (54) has the

diverging<sup>6</sup> solution [20]

$$\varrho_b(k) = \frac{1}{2\pi c_b} \sqrt{K_b^2 - k^2}. \quad (58)$$

This zero-order result corresponds to the  $n = 0$  limit of  $\varrho(k)$ , which is a well-defined expression according to the mapping between the two models, and given by

$$\lim_{n \rightarrow 0} \varrho(k) = \frac{1}{2\pi} \frac{T^3}{g\Delta} \sqrt{K^2 - k^2}, \quad (59)$$

with  $K = 2\sqrt{g\Delta\rho/T^3}$ . This result coincides with that obtained in Ref. [8] by solving an integral equation which itself is valid for  $n = 0$  only. Using Eqs. (54), (55) one gets  $K_b = 2\rho\gamma^{1/2}$ ,  $e(\gamma) = \gamma$  and, therefore, the non-trivial (disorder dependent) part of the disorder averaged free energy of the lines is given by

$$[F]_d = \lim_{n \rightarrow 0} \frac{E_0(n)}{n} L = \frac{\Delta}{2T} \left( \frac{1}{12} \frac{g\Delta}{T^3} \rho + \rho^2 \right) WL, \quad (60)$$

using Eqs. (10), (50), (57), and the correspondences of parameters in Table 2. Note the difference from the case without random potential, in which the non-linear term in  $[F]$  is proportional to  $\rho^3$ .

## 5 Distribution of the free energy in the dilute limit

The preceding Section demonstrates how the lowest order term in the energy of the Bose gas yields the first moment or cumulant of the free energy of the random line system in the limit  $\rho \rightarrow 0$ . As discussed in connection with a scaling hypothesis for PDF's of disordered system [34,17], cumulants of the free energy are also singular at critical points. To calculate these cumulants the complete  $n$  dependence of the replica free energy  $F_n$  is needed. Due to the mapping between replicated lines and bosons,  $F_n$  can be obtained order by order around  $n = 0$  by perturbation theory for the Bose gas in the weak coupling limit  $c_b = n^2 g\Delta/T^3 \ll 1$ . As realized by Lieb and Liniger [20], and as the zero-order solution [see Eq. (58)] suggests, the complete solution of the integral equation (54) is highly singular at  $c_b = 0$ . The physical meaning of this singularity in the context of the line system is related to the relevance of the random potential. Any randomness, however weak, leads to a glassy state that is fundamentally different from the pure case.

<sup>6</sup> The divergence is related to the fact that as  $c_b \rightarrow 0$  the kernel of the integral equation is a representation for  $2\pi\delta(k)$  leading to  $2\pi\varrho_b(k) - 1 \rightarrow 2\pi\varrho_b(k)$ . Therefore,  $\varrho_b(k)$  has to grow unbounded in this limit.

The singular behavior of the integral equation seems to preclude any direct analytical way of extracting higher order corrections to the zero-order result. Fortunately, for small  $\gamma$ , Bogoliubov's perturbation theory [35] can be used to calculate the ground state energy of the Bose gas. One reason for trusting Bogoliubov's theory for small  $\gamma$  is that in the case of a delta-function potential the ground state energy is given correctly by this theory in the limit of *high* boson density  $\rho$  [20]. Note that the important small  $n$  limit maps onto the high density limit of the Bose gas as far as the coupling strength  $\gamma \sim n^2/\rho$  is concerned, although we are studying the low density limit of the line system. Indeed, agreement between the exact ground state energy obtained numerically from the integral equation (54) and Bogoliubov's first-order perturbation theory has been confirmed for small  $\gamma$  by Lieb and Liniger [20]. Later Takahashi [31] used the correlated basis function method to calculate the second-order correction to the ground state energy, which again coincides with the second-order energy in Bogoliubov's perturbation theory [36], and is in perfect agreement with a numerical high-accuracy solution of the integral equation (54) down to  $\gamma \sim 10^{-5}$  [37]. Using the analytical results for first and second order terms, the next two orders can be obtained by this numerical solution, and the ground state energy summarized, in terms of the rescaled function introduced in Eq. (57), as

$$e(\gamma) = \gamma - \frac{4}{3\pi}\gamma^{3/2} + \left(\frac{1}{6} - \frac{1}{\pi^2}\right)\gamma^2 + b_5\gamma^{5/2} + b_6\gamma^3 + \mathcal{O}(\gamma^{7/2}), \quad (61)$$

with numerical coefficients [37]

$$b_5 = -0.001588, \quad b_6 = -0.000171. \quad (62)$$

It is interesting to note that the ground state energy is non-analytic in the coupling strength and thus has to be considered as an asymptotic expansion for small  $\gamma$ .

The replica free energy  $F_n$  of the line system can now be evaluated by applying the mapping between bosons and lines. First, we note that Eq. (61) provides an explicit proof that  $F_n$  is indeed an analytic function of  $n$  since  $\gamma \sim n^2$ . While this property of  $F_n$  is usually assumed in replica theories, it cannot be proved in most cases, and had not been checked before for random line lattices. In terms of the cluster size

$$l_d = \frac{1}{c} = \frac{T^3}{g\Delta}, \quad (63)$$

which sets the crossover length scale from pure to disorder dominated behavior for a single line [8], the disorder dependent part of the replica free energy can

be written as

$$F_{n,d} = \frac{LW}{l_d^2} \frac{\Delta}{2T} \left\{ \frac{n}{12} (1 - n^2) l_d \rho + n (l_d \rho)^2 - \frac{4}{3\pi} n^2 (l_d \rho)^{3/2} + \left( \frac{1}{6} - \frac{1}{\pi^2} \right) n^3 l_d \rho + b_5 n^4 (l_d \rho)^{1/2} + b_6 n^5 + \mathcal{O}(n^6) \right\}, \quad (64)$$

in the dilute limit  $\rho \ll l_d^{-1}$ . This exact result for the replica free energy has the scaling form

$$F_n = LWn \frac{\Delta \rho^2}{T} \mathcal{G} \left( n (l_d \rho)^{-1/2} \right), \quad (65)$$

where  $\mathcal{G}(x)$  is a polynomial. This result is in agreement with dimensional arguments given in Ref. [8], which motivated a scaling theory for cumulants of thermodynamic quantities in random systems [17]. Thus this scaling theory is strikingly confirmed by our exact results.

The cumulants of the free energy of the line lattice at fixed density  $\rho$  can be read off from  $F_n$ . They can be written in the general form

$$[F^p]_c = \sigma_p \frac{WL}{l_d^2} \Delta T^{p-2} (l_d \rho)^{(5-p)/2} \quad (66)$$

with coefficients

$$\sigma_1 = \frac{1}{2}, \quad \sigma_2 = \frac{4}{3\pi}, \quad \sigma_3 = \frac{1}{4} - \frac{3}{\pi^2}, \quad \sigma_4 = 0.01906, \quad \sigma_5 = -0.01026. \quad (67)$$

Consistent with the central limit theorem all cumulants of the free energy *density* vanish in the thermodynamic limit as  $[f^p]_c \sim (LW)^{1-p}$ . However, for a large but finite system the cumulants are finite and show a non-trivial dependence on the density, or on the chemical potential  $\mu$  within a grand canonical description. Close to the critical point we have  $\rho \sim \mu - \mu_c$  and  $[f^p]_c \sim (\mu - \mu_c)^{(5-p)/2}$ . Therefore, as  $\mu \rightarrow \mu_c+$  the first four cumulants vanish continuously at the critical point, the fifth cumulant approaches a constant and higher order cumulants show increasing divergence<sup>7</sup>.

Of course, since we are discussing finite systems, the singular behavior is cutoff when the correlation length approaches the system size. Due to the anisotropy of the line system, there are two correlation lengths. The first one is given by the mean distance between lines,  $\xi_{\perp} = 1/\rho$ , whereas the second one is set by the mean longitudinal distance between collisions of lines,  $\xi_{\parallel} = (gT/\Delta)^{1/2} \xi_{\perp}^{3/2}$ .

<sup>7</sup> A numerical solution of the integral equation (54) indicates that the coefficient  $b_7$  in Eq. (61) is negative and about one order of magnitude smaller than  $b_6$  [37]. This suggests that the sixth and presumably all higher cumulants have indeed non-vanishing contributions  $\sim WL$ .

The critical regime corresponds to  $\xi_{\perp} \gg W$ ,  $\xi_{\parallel} \gg L$ . We consider a fixed ratio of longitudinal and transversal system sizes so that they are in agreement with the anisotropic scaling of the system, i.e.,  $L = \delta \xi_{\parallel} (W/\xi_{\perp})^{3/2}$ , allowing for an anisotropy parameter  $\delta$ . In the critical regime, the moments of the free energy density are then given by  $[f^p]_c = \sigma_p (\Delta/TW^2)^p$  yielding *universal* relative cumulants

$$\frac{[f^p]_c}{[f]^p} = 2^p \sigma_p \delta^{1-p}, \quad (68)$$

which depend only on the geometry of the system via the anisotropy parameter  $\delta$ . This result is a consequence of the relevance of disorder, and demonstrates the complete destruction of self-averaging at the critical point, since otherwise the relative cumulants vanish with increasing system size [34]. Numerical simulations for systems of appropriate size ratios should be suitable to test this universality. Another interesting property of the PDF of the free energy is its asymmetry. Since the third and fifth cumulant are both negative, there is a higher probability for the system to be in a state with a free energy which is *smaller* than the average value. This asymmetry gets more pronounced as the system gets closer to the critical point.

Some comments on the above results for the PDF are in order. These comments are of more general nature, and are given here in order to clarify the status of the replica method itself. The replica approach provides a tool to calculate integer moments  $[Z^n]$  of the partition function. However,  $Z$  itself is unphysical, and the desired PDF of  $\ln Z$  has to be deduced using analytical continuation of the moments  $[Z^n]$  to non-integer  $n$ , and applying the cumulant series representation in Eq. (10). There are two potential problems related to this kind of procedure. First, a unique PDF can be deduced from the integer moments of the PDF only if the  $[Z^n]$  grow slower than  $n!$  for *large*  $n$  [38]. One might conclude that this condition is not fulfilled for the random line system because of  $[Z^n] \sim \exp(-E_0(n)L/T)$  and  $E_0(n)$  has a contribution proportional to  $n(1-n^2)$ , see Eq. (50). The origin of this contribution can be traced back to the energy of individual clusters in the Bethe ansatz. Therefore, the same situation appears for the single line system. In this context, it has been noted that the result for  $E_0(n)$  given above is not expected to be valid for arbitrarily large  $n$  [39]. One is led to this conclusion by the observation that the cluster size goes to zero if  $n$  tends to infinity, reflecting the tendency of *attractive* bosons to collapse. The issue of an attracting 1D Bose gas has been discussed briefly by Lieb and Liniger [20] in connection with their Bethe ansatz solution. They conclude that for the attractive Bose gas it is not clear that the Bethe ansatz wavefunction which includes the  $n$ -string solution exhausts all solutions of the Schrödinger equation. When the cluster size  $l_d$  goes to zero, it seems to be no longer justified to construct the wavefunction as a product of only two-particle functions  $\exp(-|x_1 - x_2|/l_d)$ , as done for the  $n$ -string, since they are extremely localized. The second potential difficulty of

the replica method has its origin in the order in which the thermodynamic limit and the  $n \rightarrow 0$  limit are taken. To apply the cumulant series in Eq. (10), we must expand the analytically continued function  $\ln[Z^n]$  around  $n = 0$  for a *fixed* system size. However, in calculating  $[Z^n]$  in terms of the quantum system, first we consider at *fixed*  $n$  the thermodynamic limit to eliminate all excited states. For a single line in random media the two limits do not commute due to the non-trivial sample-to-sample variation of the free energy [39], and the free energy cumulants have to be obtained indirectly by a scaling ansatz for the replica free energy [17]. For the line lattice considered here, the situation is different. Now, the extensive replica free energy  $F_n$ , obtained by first taking the thermodynamic limit and then the limit of small  $n$ , has contributions at any order in  $n$ , and thus the two limits are more likely to commute.

Finally, we would like to mention that our mapping between bosons and elastic lines provides also new information about the weak coupling limit of the ground state energy of the one-dimensional Bose gas. Since cumulants  $[F^p]_c$  of even order  $p$  have to be positive, all coefficients of non-integer powers of  $\gamma$  in the expansion of the ground state energy in Eq. (61) have to be negative, see Eq. (10). This is an important constraint on the various approximative methods in use for the Bose gas. Recently, different self-consistent approximations have been used to calculate the ground state energy based on a so-called local-field correction approach [40,41]. In view of the fact that the two approaches give different signs for the  $\gamma^{7/2}$  term in Eq. (61), our sign constraint rules out the solution of Ref. [40] from being correct.

## 6 Correlation functions

The preceding study of the free energy of the line lattice shows that disorder induces critical behavior which is distinct from the pure case. Moreover, disorder is expected to lead to correlations in the system which are different from pure 2D line lattices. In the context of flux lines in high- $T_c$  superconductors, Fisher predicted a “vortex glass” phase in which disorder locks the flux lines into one of many possible metastable states [42]. He showed that the random line lattice can be mapped onto the two-dimensional random-field XY (RFXY) model with vortices excluded. The correlation functions of the low temperature phase of the RFXY model, and the vortex glass phase, and their collective excitations have been studied extensively during the last decade. For the RFXY model, analytical approaches include replica-symmetric renormalization group (RG) techniques [43–45], and one-step replica-symmetry breaking variational ansätze [46] and RG methods [47,48]. The analytical studies of the random line lattice are mainly based on RFXY model results. They consist in scaling arguments [49], linear continuum elasticity models [50], RG techniques [51–53], and variational methods including replica-symmetry breaking [53] and

without use of replicas [54]. However, the results obtained within the different approaches are not consistent. Whereas all variational methods predict for the continuum displacement field  $u(x, y)$  of the lines, correlations of the form  $[\langle (u(x, y) - u(0, 0))^2 \rangle] \sim \ln(x^2 + y^2)$ , RG approaches yield additional corrections growing as  $\ln^2(x^2 + y^2)$ , which vanish as the non-glassy high-temperature phase is approached. A critical comparison of the various results is given in Ref. [55]. One should also keep in mind the range of validity of the different approaches. The variational methods are expected to hold throughout the whole glassy phase, while the RG results are applicable only close to the glass transition point.

Numerical simulations of glassy line lattices in two dimensions are also inconclusive. For both the variational method predictions [56,57], and the RG results [58–61], qualitative agreement was found in simulations. The numerical calculations are either hampered by slow glassy dynamics, and/or by a large length scale for the crossover to a regime where differences between the two analytical methods become significant. More recently, Zeng *et al.* [62] found good quantitative agreement, albeit in the vicinity of the glass transition, between the RG results and their numerical studies of the correlation functions via a mapping to a discrete dimer model with quenched disorder.

The analogy between the line lattice and the quantum model of  $U(n)$  fermions has been used as an alternative to RG for obtaining information about correlations in the glassy phase [15,16]. References [15] and [16] both use the replica-symmetric Bethe ansatz, but employ different techniques in handling the  $n \rightarrow 0$  limit, and make different assumptions. As a consequence, the two approaches yield different results for the asymptotic decay of the line lattice density-density correlation function, i.e.,  $[\langle \rho(x, y)\rho(0, 0) \rangle] - \rho^2 \sim (x^2 + y^2)^{-1}$  [15] compared to  $[\langle \rho(x, y)\rho(0, 0) \rangle] - \rho^2 \sim (x^2 + y^2)^{-1/2}$  [16]. Although the decay exponent of the first result is in agreement with the variational ansätze, the amplitude calculated in Ref. [15] does not agree with them. Neither result shows the logarithmic corrections predicted by the RG approaches.

In this section we reconsider the displacement and density correlations in the glassy phase by exploring the mapping of the random line lattice to the pure Bose gas. While the free energy of the former is related to the ground state energy of the latter, correlations in the statistical system are related to the low energy excitations of the quantum problem. Therefore, we calculate the low-energy excitations of the  $U(n)$  fermion model in the limit  $n \rightarrow 0$ . In the following, we consider only replica-symmetric or color-less excitations, which do not break apart the  $n$ -particle clusters corresponding to the bosons. This restriction is motivated by the fact that for  $n > 1$  only singlet states are expected to be gap-less [63], due to the finite energy associated with breaking up a cluster. With this assumption, the excitations above the ground state

consist of “cluster-particles” and “cluster-holes.” Under the mapping<sup>8</sup> of the replicated lines or  $U(n)$  fermions to the Bose gas, these excitations become the usual particle and hole states studied by Lieb [20]. He calculated the double spectrum associated with particle and hole elementary excitations exactly by Bethe ansatz. Particle states can be excited with any momentum  $p$ , but the hole state spectrum exists only for momenta  $p$  satisfying the condition  $|p| \leq \pi\rho$ . Both spectra have in common a *linear* dispersion relation at small momenta with the same velocity of sound,

$$\epsilon_{\text{p,h}}(p) = v_s |p| + \mathcal{O}(p^2), \quad (69)$$

where  $v_s$  in the weak coupling limit is given by

$$v_s = \frac{\hbar\rho\gamma^{1/2}}{m_b} = \sqrt{\frac{2\rho c_{0,b}}{m_b}}. \quad (70)$$

Since under the mapping both  $c_{0,b} \sim n$  and  $m_b \sim n$ , the excitation spectra of the replicated lines or  $U(n)$  fermions remain linear in the  $n \rightarrow 0$  limit, and the velocity of sound is given by

$$\lim_{n \rightarrow 0} v_s \rightarrow \sqrt{\frac{\rho\Delta}{gT}}. \quad (71)$$

A linear dispersion relation in the  $n \rightarrow 0$  limit was also obtained in Refs. [15,16] by solving directly a linear integral equation which determines the shifts of the Bethe ansatz momenta  $k_j$  under particle/hole excitations. However, in these references different assumptions and approximations were made to go from the excitation spectra to the density-density correlation function of the line lattice, leading to contradictory results.

Having the mapping to the pure Bose gas at hand, it is tempting to reanalyze the density-density correlations of the line lattice from a new perspective. Below we will show that the mapping gives direct results only for certain correlations in the replicated system, from which information about correlations in the original random system has to be deduced. Therefore, the remaining part of the section is guided more by the question of how much we can learn about the correlations in the line system from the knowledge of the density correlation function of the Bose gas, rather than giving final exact results for the line lattice correlations. The density-density correlation function of the 1D Bose gas at zero temperature has been studied extensively by several methods in the past, see, e.g., Ref. [33]. Since the dispersion relation is linear for small  $p$ , conformal field theory (CFT) can be employed to obtain the asymptotics

<sup>8</sup> That the mapping holds also for the excitation spectrum follows from the fact that the response of the Fermi sea (shifts of the discrete wave vectors  $k_j$ ) to excitations is completely determined by the phase shifts in an infinite system associated with transposing two wave vectors of the Bethe wave function, see, e.g., Ref. [20].

of the correlation function. The decay exponent  $\eta_b$  is given by the conformal dimensions, which are determined by the spectra of low-lying excitations. For the class of Luttinger liquids, including the Bose gas, the CFT approach is equivalent to Haldane's effective harmonic fluid description of 1D quantum fluids [32]. This description is based on the fact that the elementary excitations may be regarded as bosons which represent long-wavelength density fluctuations. The Hamiltonian for these bosons can be expressed as a sum of harmonic oscillators. Therefore, correlation functions can be calculated by simple Gaussian averages. In particular, from the Luttinger liquid approach and CFT, the asymptotic time-dependent correlation function of the local density  $b(x, t)$  of the 1D Bose gas is known at any coupling strength  $c_b$  as [32,64]

$$\langle b(x, t)b(0, 0) \rangle = \rho^2 - \frac{\eta_b}{4\pi^2} \frac{x^2 - v_s^2 t^2}{(x^2 + v_s^2 t^2)^2} + A \frac{\cos(2\pi\rho x)}{(x^2 + v_s^2 t^2)^{\eta_b/2}} + \text{h.h.}, \quad (72)$$

where the coefficient  $A$  is not known exactly and higher harmonics (h.h.) are not shown explicitly. The coupling strength enters the exponent  $\eta_b$  only via the velocity of sound, which is known perturbatively for small  $c_b$ , and numerically for all  $c_b$ , from the Bethe ansatz [20]. This exponent also determines the amplitude of the homogeneous part of the correlations, and is given by

$$\eta_b = \frac{2\pi\hbar\rho}{m_b v_s}. \quad (73)$$

We now examine to what extent the knowledge of the density-density correlation functions of the Bose gas provides information about the random line lattice correlations. First consider the correlation function of the replicated  $U(n)$  fermion system of mean density  $n\rho$ . Its local particle density  $r(x, y)$  is given by the sum over all densities  $\rho_\alpha(x, y)$  of particles of a specific color  $\alpha$ , i.e.,

$$r(x, y) = \sum_{\alpha=1}^n \rho_\alpha(x, y). \quad (74)$$

Since all replicas or colors are equivalent, we obtain in terms of the density fluctuations  $\delta\rho_\alpha(x, y) = \rho_\alpha(x, y) - \rho$ , the relation

$$\langle r(x, y)r(0, 0) \rangle = n^2\rho^2 + n\langle\delta\rho_\alpha(x, y)\delta\rho_\alpha(0, 0)\rangle + n(n-1)\langle\delta\rho_\alpha(x, y)\delta\rho_\beta(0, 0)\rangle. \quad (75)$$

On length scales larger than the cluster size  $l_d$ , see Eq. (63), the simple relation  $r(x, y) = nb(x, y)$  between boson and  $U(n)$  fermion densities holds, since

bosons correspond to  $n$ -clusters of fermions. Thus, we obtain

$$\begin{aligned} \langle b(x, y)b(0, 0) \rangle &= \rho^2 + \frac{1}{n} (\langle \delta\rho_\alpha(x, y)\delta\rho_\alpha(0, 0) \rangle - \langle \delta\rho_\alpha(x, y)\delta\rho_\beta(0, 0) \rangle) \\ &\quad + \langle \delta\rho_\alpha(x, y)\delta\rho_\beta(0, 0) \rangle, \end{aligned} \quad (76)$$

where we have assumed that all off-diagonal correlations ( $\alpha \neq \beta$ ) are identical. The disorder and thermally averaged density-density correlation function of the original line system can be calculated by taking the  $n \rightarrow 0$  limit of one of the  $n$  equivalent correlation functions for particles of the same color,

$$[\langle \rho(x, y)\rho(0, 0) \rangle] = \lim_{n \rightarrow 0} \langle \rho_\alpha(x, y)\rho_\alpha(0, 0) \rangle. \quad (77)$$

Can we extract information about this correlation function from the Bose gas correlations? Assuming that correlations of the density fluctuations  $\delta\rho_\alpha(x, y)$  have a finite limit for  $n \rightarrow 0$ , it follows from Eq. (76) that we can expect two types of terms in the  $n \rightarrow 0$  limit of Eq. (72): Contributions diverging as  $\sim 1/n$ , and those which saturate. Counting powers of  $n$  shows that we cannot identify the diagonal correlations needed in Eq. (77), but only the difference between diagonal and off-diagonal correlations. However, this difference can be calculated both in the RG approach and the variational ansatz (VA), and is therefore of interest, too. To check for the diverging contributions proportional to  $1/n$  in Eq. (72), we have to map the Bose gas exponent  $\eta_b$  to the corresponding exponent  $\eta$  of the replicated line lattice. Using the result of Eq. (71) for the mapped velocity of sound,  $\hbar \rightarrow T$  and  $m_b \rightarrow ng$ , we get in the limit  $n \rightarrow 0$  the diverging exponent

$$\eta = \frac{2\pi}{n} \sqrt{\frac{\rho T^3}{g\Delta}} = \frac{2\pi}{n} \sqrt{l_d \rho}. \quad (78)$$

For the last expression, we have used the definition of the length scale  $l_d$  given in Eq. (63). Focusing on the homogeneous part of the line density correlations, we obtain, by comparing the diverging part proportional to  $1/n$ , the correlation function

$$[\langle \rho_\alpha(x, y)(\rho_\alpha(0, 0) - \rho_\beta(0, 0)) \rangle] = -\frac{\rho^2}{2\pi} \sqrt{l_d \rho} \frac{(x/a)^2 - (y/\xi_\parallel)^2}{((x/a)^2 + (y/\xi_\parallel)^2)^2} + \text{o.t.}, \quad (79)$$

where o.t. stands for omitted oscillating terms. The length scales in the last expression are  $a = 1/\rho$ , the mean separation of lines, and  $\xi_\parallel = \sqrt{gT/\rho^3\Delta}$  corresponding to  $1/\rho v_s$ , the mean longitudinal distance between collisions of lines.

Before we discuss the oscillating contributions of the correlation function, we would like to compare our result for the difference correlations in Eq. (79) with the predictions made by RG techniques and VA. Both, RG and VA are constructed on the basis of linear elasticity theory, which describes the line

lattice in terms of a scalar displacement field  $u(x, y)$ . To represent the coupling of the random potential to the line density in terms of the displacement field, the line density in each replica  $\alpha$  has to be decomposed into harmonics as [32,65,50]

$$\rho_\alpha(x, y) = \rho \{1 - \partial_x u_\alpha(x, y)\} \sum_{m=0}^{\infty} \cos\{2\pi m \rho(x - u_\alpha(x, y))\}. \quad (80)$$

In this representation, higher order terms in  $\partial_x u_\alpha(x, y)$  are usually ignored since  $u_\alpha(x, y)$  varies slowly on coarse-grained scales. By retaining only the coupling of the first harmonic ( $m = 1$ ) to the random potential, one obtains for the displacement field  $u(x, y)$  the Hamiltonian of the RFXY model [42]. For this model, the RG approach [44] gives the result

$$\langle [\partial_x u_\alpha(x, y) \partial_x u_\alpha(0, 0)] \rangle = \frac{\partial^2}{\partial x^2} \frac{a^2}{4\pi^2} \left\{ \frac{T}{2\pi J} \ln(r/a) + \tau^2 \ln^2(r/a) \right\}, \quad (81)$$

$$\langle [\partial_x u_\alpha(x, y) \partial_x u_\beta(0, 0)] \rangle = \frac{\partial^2}{\partial x^2} \frac{a^2}{4\pi^2} \tau^2 \ln^2(r/a), \quad (82)$$

where the  $\ln^2$  contribution is obtained by an expansion to lowest order in  $\tau = 1 - T/T_g$  which measures the distance from the glass transition at  $T_g = 4\pi J$ . Here  $J$  is the elastic constant of the (isotropic) RFXY model and  $r^2 = x^2 + (c_{11}/c_{44})y^2$  the rescaled squared distance.  $J$  can be expressed in terms of the elastic constant  $c_{11}$  and  $c_{44}$ , which are related to compressions and tilts of the line lattice, by [50,55]

$$J = \frac{a^2}{4\pi^2} \sqrt{c_{11}c_{44}}. \quad (83)$$

In contrast, VA [53] yields a simple logarithmic growth of displacements with  $\tau = 0$ . The amplitude of the logarithm in Eq. (81) then depends on whether one allows for replica symmetry breaking or not. The replica symmetric result for the amplitude agrees with the RG result in Eq. (81), as compared to the universal amplitude  $a^2/2\pi^2$ , which is obtained in case of replica symmetry breaking.

The relation between density-density correlations and displacement correlations follows from Eq. (80) as

$$\langle [\rho_\alpha(x, y) \rho_\beta(0, 0)] \rangle = \rho^2 (1 + \langle [\partial_x u_\alpha(x, y) \partial_x u_\beta(0, 0)] \rangle) + \text{o.t.}, \quad (84)$$

where we have not written explicitly the oscillatory contributions which are generated by harmonics of order  $m > 1$  in the density decomposition. Using this relation, we can extract displacement correlations from our Bethe ansatz

result in Eq. (79). Comparing Eq. (79) and Eq. (84), we deduce

$$[\langle \partial_x u_\alpha(x, y)(\partial_x u_\alpha(0, 0) - \partial_x u_\beta(0, 0)) \rangle] = \frac{\partial^2}{\partial x^2} \frac{a^2}{2\pi} \sqrt{l_d \rho} \ln \left( \frac{x^2}{a^2} + \frac{y^2}{\xi_\parallel^2} \right)^{1/2}. \quad (85)$$

To complete the comparison with RG and VA, the elastic constants have to be determined in the low density limit  $\rho \ll 1/l_d$ , where the above prediction holds. The tilt modulus is given by  $c_{44} = g/a$ , whereas the compression modulus  $c_{11}$  is determined by the mutual interaction potential  $W(x)$  of the lines. Due to entropic and steric repulsions, the original contact potential becomes long-ranged. The interaction potential can be read off from the free energy density  $f(a = 1/\rho)$  since in a grand-canonical description with chemical potential  $\mu$  one has

$$f(a) = \{-g(\mu/\mu_c - 1) + W(a)\}/a. \quad (86)$$

The elastic constant  $c_{11}$  is now determined by the curvature of the free energy density, evaluated at the mean line separation  $a$ , as

$$c_{11} = x^2 f''(x)|_{x=a} = aW''(a) = \frac{\Delta}{Ta^2}. \quad (87)$$

To calculate the last expression, which is valid in the low density limit  $a \gg l_d$ , we have used the result for the free energy in Eq. (60), which yields the non-trivial part  $W(a)/a$  of the free energy density. From this result for the elastic constants we obtain  $J = (ag\Delta/T)^{1/2}/4\pi^2$ , and hence the amplitude of the ln term of the RG result in Eq. (81) becomes

$$\frac{a^2 T}{8\pi^3 J} = \frac{a^2}{2\pi} \sqrt{l_d \rho}, \quad (88)$$

which is in complete agreement with the Bethe ansatz result of Eq. (85). Moreover, there is also agreement between the two results regarding the anisotropy parameter, since  $\xi_\parallel = (gT/\rho^3 \Delta)^{1/2} = a(c_{44}/c_{11})^{1/2}$  in the dilute limit. This means that the velocity of sound is related to the elastic constants by the mapping between bosons and replicated lines according to

$$\left( \frac{c_{11}}{c_{44}} \right)^{1/2} \longleftrightarrow v_s. \quad (89)$$

It is interesting to note that exactly the same relation holds in the case of a *pure* 1 + 1-dimensional line lattice, which can be mapped to world-lines of *free* fermions [14] with  $v_s = \pi \hbar \rho / m \leftrightarrow \pi T \rho / g$ .

Compared to the VA, our Bethe ansatz result for the difference correlations  $[\langle \partial_x u_\alpha(x, y)(\partial_x u_\alpha(0, 0) - \partial_x u_\beta(0, 0)) \rangle]$  is only in agreement with the replica symmetric case. A universal amplitude of the logarithm as predicted by the

VA with replica symmetry breaking is not reproduced by our approach. However, the agreement of the Bethe ansatz result with the RG predictions is not complete. If the RG is assumed to give the correct result, then there should appear also a slower decaying contribution proportional to  $\ln(r)/r^2$  in the Bose gas correlations in Eq. (72) which remains finite in the  $n \rightarrow 0$  limit. This contribution corresponds to the last off-diagonal term in Eq. (76), for which this slower decay follows from the RG result in Eq. (82).

There are two potential reasons for the absence of such kind of contributions in our Bethe ansatz approach. The first one is not related to our mapping, but can be traced back to the fact that there are indeed logarithmic corrections to Haldane's harmonic fluid approach for the 1D Bose gas. These corrections vanish in the strong coupling limit  $c_b \rightarrow \infty$  and have been calculated explicitly so far only in a  $1/c_b$  expansion by Korepin [66] using the quantum inverse scattering method and by Berkovich and Murthy [64,67] by means of conformal field theory. However, these results predict, in agreement with each other to first order in  $1/c_b$ , logarithmic corrections only to the oscillating term of Haldane's result in Eq. (72). Therefore these results do not account for  $\ln$  contributions to the homogeneous part of the density-density correlation function. But we are interested in the weak coupling limit  $c_b \sim n^2 \rightarrow 0$ , where the actual form of the corrections is not yet known. The second potential, and we think more likely reason for the absence of corrections is related to the fact that we apply our mapping to obtain the excitation spectra of the  $U(n)$  fermions from the Bose gas spectra by assuming that only non cluster breaking replica symmetric excitations are gap-less. This assumption is certainly justified for integer  $n$  due to the finite energy necessary to break up a cluster. But if  $n$  goes to zero, cluster breaking excitations might become gap-less, providing a possible source of additional contributions to the asymptotic density-density correlations. Note that these cluster breaking excitations can be absolutely replica symmetric since  $n$  particles of mutual different colors can be transferred from different clusters across the Fermi surface to form together a color neutral excitation. Taking into account this type of excitations is, of course, very interesting<sup>9</sup>, but not possible within the mapping to bosons, which itself cannot be broken apart.

Finally, we come back to the oscillating term in the Bose gas correlation function of Eq. (72), and its implications for the correlations in the line lattice. This term and higher harmonics are quite important in view of experimental determinations of the translational order of line lattices. Scattering experiments measure the Fourier transform of the density-density correlation function around a reciprocal lattice vector  $2\pi m\rho$  with integer  $m$ . Therefore, these experiments can determine the value of the line lattice analogue  $\eta$ , of the ex-

---

<sup>9</sup> The splitting of clusters has been considered by Parisi for a single line ( $N = 1$ ) to study the possibility of replica symmetry breaking [68].

ponent  $\eta_b$  of the Bose gas correlations. Using the mapping between lines and bosons, we have seen that  $\eta_b \sim 1/n$  [see Eq. (78)] and therefore

$$\eta \rightarrow \infty, \tag{90}$$

in the  $n \rightarrow 0$  limit. This result is in strong contrast to the case of a *pure* line lattice with  $\eta = 2$ . The infinite exponent means that the oscillating terms in the density correlation function decay faster than any power law due to destruction of quasi-long-range order by the random potential. Exactly the same result was obtained by Cardy and Ostlund in their RG approach [43], but it is in contradiction to all VA approaches. Although a mean squared relative displacement which grows slightly faster than a logarithmic increase cannot be obtained directly from the homogeneous part of the Bose gas density correlations, the fact that the Bose gas exponent  $\eta_b$  is mapped onto an infinite  $\eta$  for the line lattice might be interpreted as a signature of the presence of these contributions. However, this argument has to be viewed with care since  $\eta \sim 1/n$  means that the oscillating terms of the density-density correlation function have an essential singularity in the  $n \rightarrow 0$  limit.

## 7 Conclusion and discussion

In this paper, we studied the probability distribution function of the free energy of a lattice of lines, distorted due to thermal and disorder fluctuations. Using the replica approach in combination with an analytically continued nested Bethe ansatz, we calculate exactly the cumulants of the free energy in the dilute limit. Our results confirm a previously proposed scaling form for the replica free energy in terms of the replica number  $n$ , as a scaling field [17]. These exact results were obtained by establishing a novel analogy between the random line lattice and the weakly interacting 1D Bose gas with delta-function interactions. Based on this analogy, we related the results for the density-density correlation function of the Bose gas, known from Haldane's effective theory of 1D quantum liquids, and from conformal field theory, to correlation functions of the line lattice. Our result for the difference between diagonal and off-diagonal replica-correlations is in agreement with RG predictions, and a replica symmetric variational ansatz for an elastic model of the line lattice, if one takes into account the correct disorder dependence of elastic constants obtained by the Bethe ansatz approach for the free energy. The Bethe ansatz results do not agree with the variational ansatz with replica symmetry breaking. The comparison with the RG results of Cardy and Ostlund [43] and Goldschmidt and Houghton [44], which predict a faster than logarithmic growth of relative line displacements, shows that our mapping to a Bose gas cannot capture the corresponding contributions. Potential sources for these additional logarithmic terms within the Bethe ansatz provide avenues

for future explorations.

Finally, it might be interesting to note that all results obtained in this paper are valid if the length scale  $l_d$ , setting the crossover to random behavior for a single line, is much larger than the correlation length  $\xi_0$  of the random potential. When this condition is fulfilled,  $\xi_0$  does not show up in the final results, and can be safely set to zero from the beginning as we did throughout the paper, see Eq. (3). However, if temperature is decreased, the length scale  $l_d = T^3/g\Delta$  also decreases, and gets equal to  $\xi_0$  at the crossover temperature  $T^* = (\xi_0 g \Delta)^{1/3}$ , which is of the order of the smallest random energy barrier [69]. Therefore, our results apply directly to the high temperature regime  $T \gg T^*$ . They can also be extended to the low temperature limit  $T \ll T^*$ , using a method developed by Korshunov and Dotsenko [70] to calculate the replica free energy of a single line in a random potential with finite  $\xi_0$ . By splitting the  $n$ -cluster for a single line into  $n/k$  separate blocks with  $k \sim T/T^*$ , they were able to show that the ground state energy of their model with finite  $\xi_0$  can be obtained from the model with  $\delta$ -function interactions by the simple substitutions  $g \rightarrow kg$ ,  $\Delta \rightarrow k^2\Delta$  and  $n \rightarrow n/k$ . Since the internal structure of individual clusters remains unchanged by considering a finite density of clusters (see the ansätze in Eqs. (30)-(32)), our results can be translated easily to the low-temperature regime by the above substitutions.

## Acknowledgements

We would like to thank E. Frey, A. Hanke, V. E. Korepin, T. Nattermann, V. L. Prokovsky and W. Zwerger for discussions and conversations. This work was supported by the Deutsche Forschungsgemeinschaft under grant No. EM70/1-3 (T.E.), and by the National Science Foundation grants No. DMR-98-05833 and No. PHY99-07949 (M.K.).

## References

- [1] T. Halpin-Healy, Y.-C. Zhang, Phys. Rep. **254** (1995) 215.
- [2] M. Kardar, G. Parisi, Y.C. Zhang, Phys. Rev. Lett. **56** (1986) 889.
- [3] D.A. Huse, C.L. Henley, D. S. Fisher, Phys. Rev. Lett. **55** (1985) 2924.
- [4] T. Hwa, M. Lässig, Phys. Rev. Lett. **76** (1996) 2591.
- [5] T. Hwa, Nature **399** (1999) 17.
- [6] C.A. Bolle et al., Nature **399** (1999) 43.

- [7] T. Davis, J. Cardy, Nucl. Phys. B **570** (2000) 713.
- [8] M. Kardar, Nucl. Phys. B **290** [FS20] (1987) 582.
- [9] B. Derrida, H. Spohn, J. Stat. Phys. **51** (1988) 817.
- [10] D.A. Gorokhov, G. Blatter, Phys. Rev. Lett. **82** (1999) 2705.
- [11] E. Brunet, B. Derrida, Phys. Rev. E **61** (2000) 6789.
- [12] W. W. Mullins, R. F. Sekerka, J. Appl. Phys. **35** (1964) 444.
- [13] P. G. de Gennes. J. Chem. Phys. **48** (1968) 2257.
- [14] V. L. Pokrovsky, A. L. Talapov, Phys. Rev. Lett. **42** (1979) 65.
- [15] A. M. Tsvetik, Phys. Rev. Lett. **68** (1992) 3889.
- [16] L. Balents, M. Kardar, Nucl. Phys. **B393** (1993) 480.
- [17] T. Emig, M. Kardar, Phys. Rev. Lett. **85** (2000) 2176.
- [18] C. N. Yang, Phys. Rev. Lett. **19** (1967) 1312.
- [19] M. Takahashi, Prog. Theor. Phys. **44** (1970) 899.
- [20] E. H. Lieb, W. Liniger, Phys. Rev. **130** (1963) 1605; E. H. Lieb, Phys. Rev. **130** (1963) 1616.
- [21] D. R. Nelson, H. S. Seung, Phys. Rev. B **39** (1989) 9153.
- [22] R. P. Feynman, A. R. Hibbs, *Quantum Mechanics and Path Integrals* (McGraw-Hill, New York, 1965); R. P. Feynman, *Statistical Mechanics* (Benjamin, Reading, 1972).
- [23] H. A. Bethe, Z. Phys. **71** (1931) 205.
- [24] H. B. Thacker, Rev. Mod. Phys. **53** (1981) 253.
- [25] M. Gaudin, Phys. Lett. **24A** (1967) 55.
- [26] D. S. Koltun, Phys. Rev. C **36** (1987) 2047.
- [27] B. Sutherland, Phys. Rev. Lett. **20** (1968) 98.
- [28] F. G. Tricomi, *Integral Equations* (Interscience, New York, 1957).
- [29] I. S. Gradshteyn, I. M. Ryzhik, Table of Integrals, Series and Products (Academic Press, Orlando, 1980).
- [30] T. Emig, M. Kardar, in preparation.
- [31] M. Takahashi, Prog. Theor. Phys. **53** (1975) 386; *Thermodynamics of one-dimensional solvable models* (Cambridge University Press, Cambridge, 1999).
- [32] F. D. M. Haldane, Phys. Rev. Lett. **47** (1981) 1840.

- [33] V. E. Korepin, N. M. Bogoliubov, A. G. Izergin, *Quantum inverse scattering method and correlation functions* (Cambridge University Press, Cambridge, 1997).
- [34] A. Aharony, A. B. Harris, Phys. Rev. Lett. **77** (1996) 3700.
- [35] N. N. Bogoliubov, J. Phys. USSR **11** (1947) 23.
- [36] D. K. Lee, Phys. Rev. A **4** (1971) 1670; Phys. Rev. A **9** (1974) 1760.
- [37] T. Emig, M. Kardar, unpublished.
- [38] N. I. Akhiezer, *The Classical Moment Problem* (Oliver and Boyd, London, 1965).
- [39] M. Kardar, in *Fluctuating Geometries in Statistical Mechanics and Field Theory*, Proceedings, F. David, P. Ginzparg, and J. Zinn-Justin, eds. (Elsevier, Amsterdam, 1996).
- [40] A. Gold, Z. Phys. B **91** (1993) 397.
- [41] E. Demirel, B. Tanatar, Phys. Rev. B **59** (1999) 9271.
- [42] M.P.A. Fisher, Phys. Rev. Lett. **62** (1989) 1415.
- [43] J. L. Cardy, S. Ostlund, Phys. Rev. B **25** (1982) 6899.
- [44] Y. Y. Goldschmidt, A. Houghton, Nucl. Phys. B **210** (1982) 155.
- [45] M. Paczuski, M. Kardar, Phys. Rev. B **43** (1991) 8331.
- [46] S. E. Korshunov, Phys. Rev. B **48** (1993) 3969.
- [47] P. Le Doussal, T. Giamarchi, Phys. Rev. Lett. **72** (1994) 1530.
- [48] J. Kierfeld, J. Phys. I (France) **5** (1995) 379.
- [49] D. S. Fisher, M. P. A. Fisher, and D. A. Huse, Phys. Rev. B **43**, (1991) 130.
- [50] T. Nattermann *et al.*, Europhys. Lett. **16** (1991) 295.
- [51] J. Toner, Phys. Rev. Lett. **67** (1991) 2537; J. Toner, *ibid.* **68** (1992) 3367.
- [52] T. Nattermann, I. Lyuksyutov, Phys. Rev. Lett. **68** (1992) 3366.
- [53] T. Giamarchi, P. Le Doussal, Phys. Rev. B **52** (1995) 1242.
- [54] H. Orland, Y. Shapir, Europhys. Lett. **30** (1995) 203.
- [55] T. Nattermann, S. Scheidl, Adv. in Phys. **49** (2000) 607.
- [56] G. G. Batrouni, T. Hwa, Phys. Rev. Lett. **72** (1994) 4133.
- [57] D. Cule, Y. Shapir, Phys. Rev. Lett. **74** (1995) 114.
- [58] D. J. Lancaster, J. J. Ruiz-Lorenzo, J. Phys. A **28** (1995) L577.
- [59] E. Marinari, R. Monasson, and J. J. Ruiz-Lorenzo, J. Phys. A **28** (1995) 3975.

- [60] C. Zeng, A. A. Middleton, and Y. Shapir, Phys. Rev. Lett. **77** (1996) 3204.
- [61] H. Rieger, U. Blasum, Phys. Rev. B **55** (1997) R7394.
- [62] C. Zeng, P. L. Leath, and T. Hwa, Phys. Rev. Lett. **83** (1999) 4860.
- [63] I. Affleck, F. D. M. Haldane, Phys. Rev. B **36** (1987) 5291.
- [64] A. Berkovich, G. Murthy, Phys. Lett. A **142** (1989) 121.
- [65] T. Nattermann, Phys. Rev. Lett. **64** (1990) 2454.
- [66] V. E. Korepin, Commun. Math. Phys. **94** (1984) 93.
- [67] A. Berkovich, Nucl. Phys. B **356** (1991) 655.
- [68] G. Parisi, J. Phys. France **51** (1990) 1595.
- [69] T. Nattermann, W. Renz, Phys. Rev. B **38** (1988) 5184.
- [70] S. E. Korshunov, V. S. Dotsenko, J. Phys. A **31** (1998) 2591.